Aalborg University

Acoustics And Audio Technology

Augmented Acoustic Reality Realized Through Hear-Through Device

With emphasis on platform development

Author:
Christoffer Bovbjerg
Rune Egedal

Supervisor:
Flemming Christensen

June 2, 2014

Title:
  Implemented Hear Through Device

Topic:
  Master Thesis

Project period:
  Spring Semester 2014

Group:
  1060

Participants:
  Christoffer Bovbjerg
  Rune Egedal

Supervisor:
  Flemming Christensen

Pages: 109

Appendices: 5

Terminated: June 2, 2014

Synopsis:

The following is a master thesis in Acoustics and Audio Technology. The main purpose of the thesis is to develop a hear through device platform. The thesis contains theory on spatial hearing used for virtual source implementation and a complete design in software and hardware. The hardware is developed as two separate devices, a hear through device and a processing platform. The system equalization is developed based on comprehensive measurements accounting for auricular transfer functions and transducer nonlinearity. The thesis focuses on the transparency of the system. The developed platform is designed to be open and can be used for several signal processing tasks within acoustics. All subsystems of the developed platform is tested and verified. The report features a complete user's guide to the system and a template for future research in the field of hear through devices and augmented acoustic reality.

Foreword

The following master thesis was written in the spring of 2014. The reader is expected to have thorough knowledge of acoustics, signal processing and electronics. Throughout the report several references to the attached project CD are marked with the 💿 symbol followed by a relative path. This document and all its source files can be found as well in 💿`/Report/`. The appendices included contain all measurement reports and includes a user manual and electrical documentation for the entire system. All appendices are referred to with capital letters. When mentioned the hear through device only reefers to the device in the ear. Figures generated with MATLAB can be generated and inspected by running the referenced programs on the project CD.

We would like to thank the following people at AAU for their invaluable help and time:

<div align="center">

Peter Boie Jensen
Ben Krøyer
Kenneth Knirke Nielsen
Claus Vestergaard Skipper

</div>

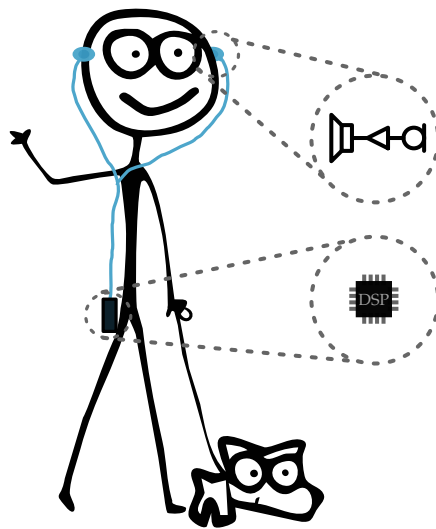<div align="center">

Christoffer Bovbjerg   **Rune Egedal**

</div>

Contents

Chapter 1

Preface

1.1 Introduction

The hear through device is a device that allows a user to listen *"through"* a headphone. It is in essence an in-ear headphone with a microphone attached on the outside. The microphone allows the device to record the sound that would normally enter the ear canal. Using the microphone signal allows sound transfer to the eardrum as if the device was absent. The applications are not discussed in this report, but several are investigated in [Härmä et al., 2003].

Familiarity with virtual reality, where the user is presented with a completely synthetic reality is fairly common. The acoustic equivalent is headphones that completely block any outside sounds. The hear through idea is augmented acoustic reality, meaning that it is a combination of reality and virtual reality. The hear though device share several properties with hearing aids, but it is not intended to alleviate hearing loss.

This master thesis concerns the development of a hear through device and an auxiliary processing platform as illustrated in the figure to the left. Simulating a three dimensional augmented acoustic reality is the main purpose of the device. The device will also serve as a development platform for future research in hear through devices and their applications. This thesis will focus on the design and implementation of the development platform and hear through device and should serve as a generic template for many use cases.

In order to create an augmented acoustic reality a system of microphones and headphones(hear through device) can be used to control the signal path to the user. Passing the signal through unchanged allows the system to be transparent to the user. Having access to the signal path allows injection of virtual sources with the directional characteristics realized using binaural synthesis. These sources however must also have the same characteristics as the microphone signal in order to blend in seamlessly. This requires the system to detect and extract critical information from the real signal, and apply this information to any virtual source. [Savioja et al., 1999]

The project is proposed by Associate Professor Flemming Christensen, the original proposal can be found at ⊘`/ProjectProposal.pdf`.

1.2   Project Description

The project aims to implement a hear-through device. This device must fulfill the following key elements:

- **Calibrated system**
  The system must accurately reproduce any sound pressure within the normal hearing range.
- **Transparrent**
  The system must allow the users normal hearing.
- **Source**
  The system must seamlessly infuse a stationary virtual source.

Several tasks arise from these three main challenges. The following chapters will systematically investigate and analyze the required parameters to acheive such a device functionality. As the device is intended for use by humans, the spatial hearing chareteristics of humans must be thoroughly analyzed. The following chapter analyze the characteristics used in localizing sound sources. The characteristics will be used as a basis to determine the system requirements for the device.

Chapter 2

Principles Of Human Sound Localization

2.1 Spatial Hearing

In the following sections the theory of source localization by humans will be investigated assuming idealized and anechoic conditions. This knowledge will be used in the implementation of the virtual sound sources. Several factors must be taken into account to implement the hear through device because of the missing characteristics of the body and outer ear when using headphones.

The first section will investigate the binaural signals which are present when both ears are used for localization. Next monaural cues are investigated. The influence of shoulder and upper body are also accounted for in this section. The third section investigates the dynamic cues such as head movements. In the fourth section the externalization of sound is investigated. The last section describe other senses and their influence on sound localization.

This part of the theory applies to sound localization of any virtual sound source created by the system. The real sound from the microphone is assumed to include all localization cues. These sections are based on the literature by [Letowski and Letowski, 2012].

2.2 Binaural Cues

As mentioned in the above, binaural cues refer to the circumstances where both ears are used and the interaural cues are used in localization. The geometry of the human head infers these cues, due to the distance and placement of the ears. The interaural cues are the Interaural Time Difference (ITD) and the Interaural Level Difference (ILD). The ITD describe the case where a sound source is located of axis and hereby introduces a difference in arrival
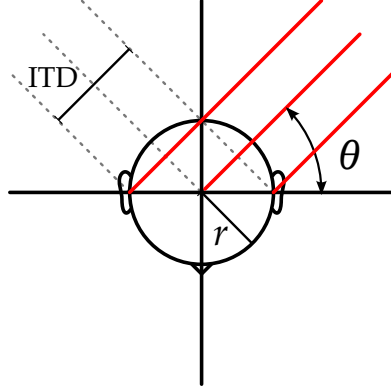
Figure 2.1: Inter aural time difference illustrated as seen form above. Red lines depict the incoming pressure wave. θ is the angle of incidence and r is the radius of the head.
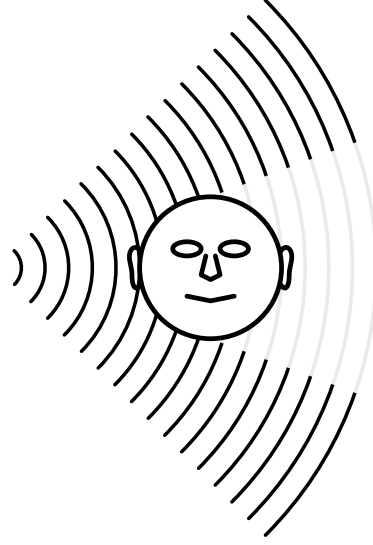
Figure 2.2: Interaural level difference as seen form the front. The wavelength is smaller than the head causing an acoustic shadow on the left ear.

times at the ears caused by the difference in distance. The ILD refers to the level difference of a sound source in [dB] at each ear. Each of these models assume a spherical head.

Interaural Time Difference

ITD describe how the geometry of the head affects the time difference between the sound arrival at each ear as illustrated in figure 2.1. The ITD has the lowest value at $\theta = 0°$ which corresponds to a sound source straight ahead of the listener. The highest value of the ITD is reached at $\theta = 90°$ which corresponds to a sound source placed either left or right of the listener. The ITD can be expressed as:

$$\text{ITD} = \frac{a \cdot r}{c} \cdot \sin \theta \tag{2.1}$$

Here r is the radius of the listeners head(sphere), θ is the angle between the listener and the sound source, c is the speed of sound. The ITD has a slight frequency dependency due to diffraction around the head at lower frequencies, and a is therefore introduced as a variable. The variable a is defined in the following way:

$$a = \begin{cases} 3 & \text{if } f < 500 \text{ Hz} \\ 2 & \text{if } f > 2000 \text{ Hz} \end{cases} \tag{2.2}$$

a's shift is monotonic over the frequency range with only minor exceptions.

Interaural Level Difference

The ILD cue is as well as the ITD based on the geometries of the human head. The ILD is an expression of the level difference of a sound source arriving at the ears as illustrated in figure 2.2. For the ILD to work as a localization cue there has to be a significant level difference at each ear. Although sound decreases in intensity, and thereby level, when traveling through air, it does not decrease significantly over a small distance, like the distance between the ears. This disqualifies the ILD as a localization cue at wavelengths larger than the head. In this case the sound level will be approximately the same at both ears. Decreasing the wavelength to be less than the head size, will introduce a level difference at the ears caused by the head blocking the sound path, creating an acoustic shadow, and thereby provide a localization cue.

Interaction Of Interaural Time Difference And Interaural Level Difference.

ITD and ILD serve as binaural cues for sound localization. The cues work together to enable localization of sound. The ITD is the most significant cue as it works well at low frequencies and can help emphasizing localization at higher frequencies. Everyday sounds such as traffic noise and speech, where localization is important, primarily contain low frequency energy which implies the ITD would be the most significant localization cue.

The Binaural cues do have their limitations. Because of the symmetry of the human head the ITD's will mirror at specific positions which will cause confusion. This makes it impossible to distinguish from which of the positions the the source originated, and the brain has to choose the right position without these cues. The confusion caused at these points of symmetry are commonly referred to as *cone of confusion* and *front back confusion*. This is a problem when using only the binaural cues.

2.3   Monaural Cues

Monaural cues describe to the circumstances where only one ear is used in order to localize the sound source. Several factors influence the monaural cues, but as with the binaural cues they are all results of the geometry surrounding the ears. The major characteristics are caused by the shoulder, upper torso, head size and the shape of the outer ear (pinna). All of the mentioned factors causes reflections which influences the sound arriving at the ear, and hereby altering the characteristics of the received sound. The effect of this can be characterized by the magnitude response of the Head-Related Transfer Function (HRTF). The major body parts such as head, shoulders

and upper torso affect the response at 2-3 kHz. Because of the relatively small dimensions in the pinna it will only have effect on frequencies above 3-4 kHz. Several studies have been performed in order to show the effects of the pinna, aside from its influence on the HRTF magnitude response. It is shown that the removal of the pinna cues decrease localization accuracy and furthermore the *outside of the head* spatial impression collapses.

By using only binaural cues, effects such as *front back confusion* are problematic. But by adding the monaural cues this problem can be reduced. The notches and peaks in the HRTF magnitude response reveal weather the sound source is located in the front or back when the binaural cues can not.

A problem to address is the individuality of the human ear. Humans do not have the same size and shape. This will yield some differences in the HRTF from one human to another. This implies that accurate localization can only be achieved with individualized HRTF's fitted to each person. Studies conducted has shown that training with a non individualized HRTF's result in the ability to localize accurately, this allows a generalized HRTF in a virtual acoustic environment [Mendonça et al., 2012].

To obtain HRTF's they have to be measured. To cover the entire pathway for the sound it would be preferable to measure the sound pressure right at the eardrum. This is however rather difficult. Studies of 40 human subjects have shown that the spatial information of the sound is not lossy when measured at a blocked ear canal. Furthermore the individuality of the measurements are not as pronounced, when the ear canal is excluded, and therefore more compatible. [Møller et al., 1995]

2.4   Dynamic Cues

The binaural and monaural cues are used as the main cues for localizing a sound source. As mentioned the confusion that can appear by use of the binaural cues can to some degree be resolved by introducing monaural cues. However by introducing the dynamic cues caused by head movements the localization can be further increased, and the confusions can be suppressed almost completely.

Head Movement

Head movements can help resolve the problem of *front back confusion* and *cone of confusion*. A simple way to realize the advantage of head movement is to place a sound source directly in front of the listener. The binaural cues from the ITD will be zero and this makes it difficult for the subject to distinguish whether the sound originates from front or back. Rotating the head will result in a longer path to one of the ears, this yields a difference in the ITD suppressing the *front back confusion*. Moving the head enables

humans to focus acoustically, this movement generates additional cues for localizing sound sources on the entire sphere around the head.

Studies of head movements and their influence on sound localization have been conducted [Blauert, 1999]. These studies all agree on the necessity of movements to decrease localization error. Furthermore it is shown that the first movement most subjects do in order to localize, is to turn their head towards the sound source, but not necessarily directly at it. An important feature of head movements is the ability to localize sound as coming from out side of the head when headphones are used to reproduce the sound [Klensch, 1948]. The study was conducted with small funnels connected to a rubber pipe that was inserted into the ear canal. Different cases were studied, eg. no head movement but movement of funnels resulting in an *inside the head* localization. The latter part of the study incorporated head movement while the funnels were in motion resulting in externalization of the sound.

Head movements help minimizing localization error to a certain degree. One aspect of the sound source which has to be fulfilled is the duration of the sound. Head movements are only useful in a certain time window. Studies have shown that for sound emitted for less than 500 ms, head movements have no significant influence on localization, but with increasing duration of the sound the advantage of the head movements increases localization.

2.5 Externalization Of Sound

When one sound source is playing in an anechoic environment all of the above mentioned cues are used in order to localize the sound. By introducing another sound source the sound will be heard as fused as long as the sound arrive at the ears at the same time. By introducing a slight delay (>1 ms) to one of the two sources, the sound will be heard as coming from the source playing first. This effect is know as the *law of the first wavefront* or the *precedence effect* and is useful as a dynamic cue even when only one source is playing. In a normal listening situation the room will add reverberation to the source, by reflecting on the floor, walls and sealing. The result of the *precedence effect* prevents reflections from confusing localization even though several reflected sources appear. The delay between the sound events will at a point ($\gtrsim 20$ ms, depending on the complexity of the sound) yield an echo and the sound will be heard as coming from two different sources.

Reverberation

An element of spatial hearing involves the environmental cues caused by reflections from surrounding surfaces. Depending on the room the listener is situated in the source will sound different. Listening to a sound source in anechoic conditions will have a *dry* sound, because only the direct sound is heard. Placing the source in a reverberant environment will give the sound a

wet character caused by a difference in arrival time and amplitude. This difference is caused by the path length difference of the reflected sound. Studies show that listening in an anechoic chamber can result in an *inside-the-head* localization of the sound [Toole, 1970]. This situation can be compared to listening with standard headphones. By using headphones the room is removed from the sound path and results in the same *inside-the-head* localization effect.

Studies of subjects ability to judge the externalization of the sound source in anechoic and reverberant rooms shows that by adding reverberation to the sound the *inside-the-head* localization effect decreases significantly. This implies a necessity for adding reverberation to any virtual source. [Begault, 1994]
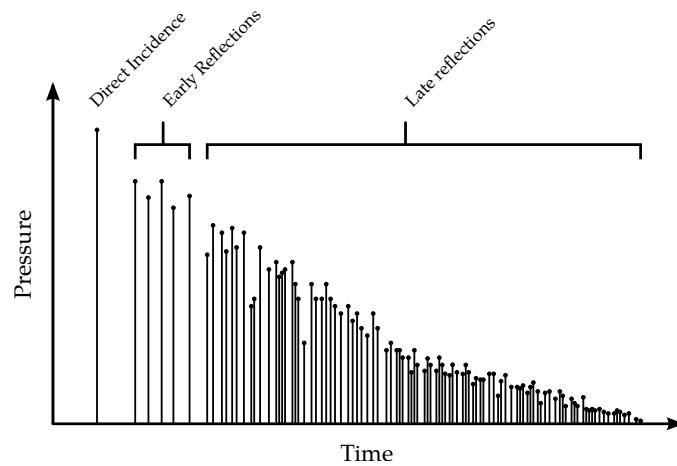

Figure 2.3: Impulse response of a room, showing the direct, early- and late reflections.

Reverberation time is generally defined as the time it takes for the sound level to decrease by 60 dB, once the source is turned off. The reverberation is dependent on the room geometry. Analyzing the impulse response characteristics of reverberation is found to always contain the direct signal, early reflections and late reflections. This characteristic is illustrated in figure 2.3. The early reflections are visible in the first part of the impulse, right after the direct sound. They are usually caused by reflections from the floor, ceiling and walls. The late reflections contains sound that has been reflected several times, resulting in a more dense response at the end of the impulse response. The first 80 ms of the reverberation is the most important to impose the sensation of a room, this value is not specific because of the dependency of the room composition, but is used as a rule of thumb. This implies that early reflections are important for the externalization of sound and late reflections have little influence on the externalization, but will give the source a more natural sound.[Begault, 1994]

2.6   Non Aural Cues

All cues described to this point are determined as aural cues. Other human senses also influence how sound sources are localized. These cues are more difficult to quantify as many of them rely on higher brain functions and are not simply a product of geometry and reflections. Vision cues are the most important of these senses as they contribute to localization and has a tendency to override the aural cues. This is also known as the *capture effect.* Studies show that if the source is visually offset up to 30° on the horizontal plane, the listener tends to chose that position rather than the actual source position [Thurlow and Jack, 1973]. The *capture effect* works as long as there is a visual impression that can be interpreted as the sound source. This is further emphasized by use of head movements which minimize localization error of *invisible* sound sources.

Besides visual cues other cues such as memory can affect localization. One example is the sound of a bird, usually the immediate localization will be somewhere in the upper hemisphere. Depending on the duration of the sound, localization will correct the impression and localize the sound source correctly.

2.7   Preliminary Studies

The cues and their implementation are crucial for the system to have the desired effect when introducing virtual sound sources. In this section the important features of the Auricular Transfer Function(ATF), will be investigated via measurements. As the system is expected to be transparent to the listener. The response of the headphone is also examined in order to reduce the influence on the HRTF's.

The measurement reports used to support the following sections can be found in appendices A, B, C and D.

Choice Of Headphones

A key element of the hear through device is that it allows full transparency through the system, allowing a listener to hear as they normally would. This means that every coloration the system adds must be dealt with. Any volume that fills the pinna will also have an impact on the listeners HRTF's. Because of this limitation the headphone should ideally be contained within the ear canal. The closest approximation available is in-ear headphones. So available headphones where evaluated to find a headphone with a very small volume. Several in-ear headphones where evaluated and can be viewed at ⊙**/Hardware/Headphones/**. AKG model K323XS was chosen, the headphone can be seen in figure 2.4.
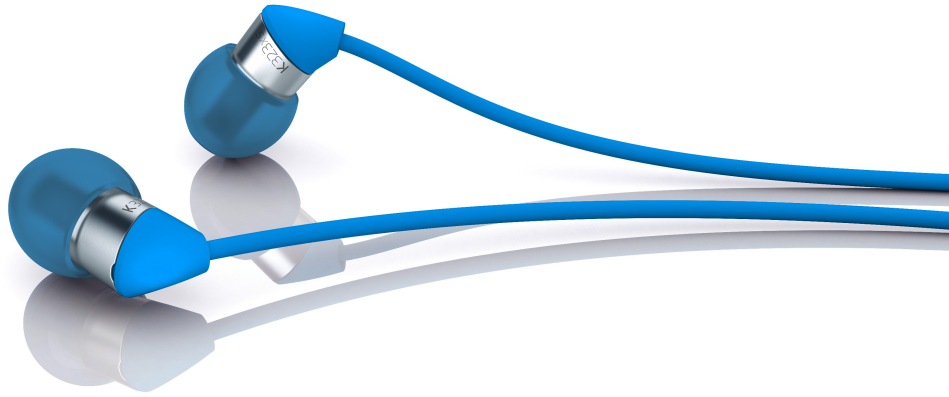
Figure 2.4: The AKG K323XS in-ear headphone chosen for the hear-through device (product photo from AKG [AKG, 2014]).

In appendix D a measurement of the in-ear headphones frequency response is performed. The measurement is conducted using a coupler with the headphone inserted. An MLS sequence was played back and the resulting impulse response is obtained and Fourier transformed to give a frequency response. As seen in figure 2.5 the characteristics of the headphone will have some influence on the signal. This response must be equalized.
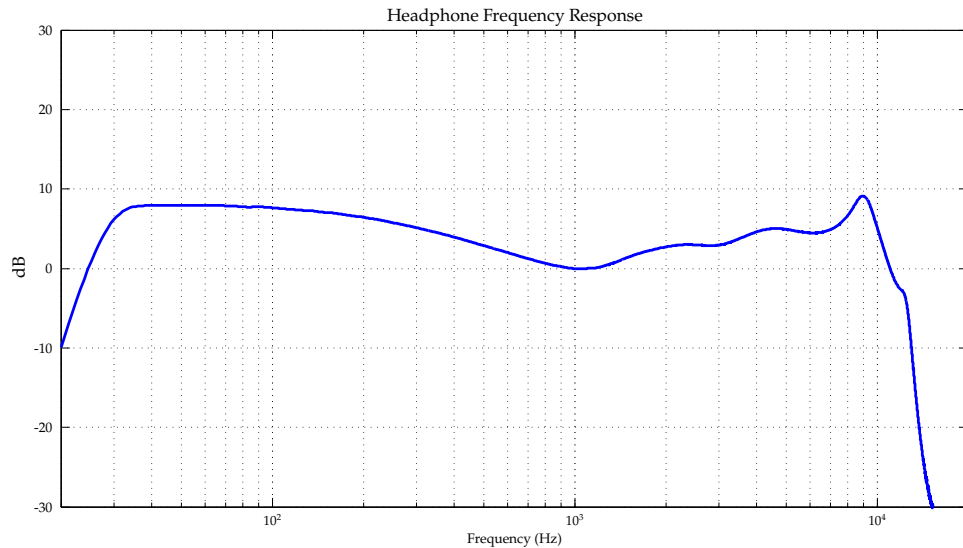

Figure 2.5: Frequency response of the AKG K323XS headphone, normalized at 1k Hz.

In appendix C the insertion loss caused by the insertion of the in-ear headphone is investigated as it is important to know how much sound leaks through the system. The test is conducted on two male subject 26 and 28 years of age with normal hearing. When wearing the headphone an average

insertion loss of 23.2 dB was determined. The sound that will leak through the device is attenuated and the influence of this should be insignificant at normal sound levels. A more detailed view of the results is seen in the audiometry in figure 2.6. Even though the average insertion loss is determined to 23.2 dB the loss varies quite a bit depending on frequency. The insertion loss at low frequencies is not significant which implies that low frequencies will to some extend be transmitted to the listener. This characteristic will have influence on the development of filters for equalizing.
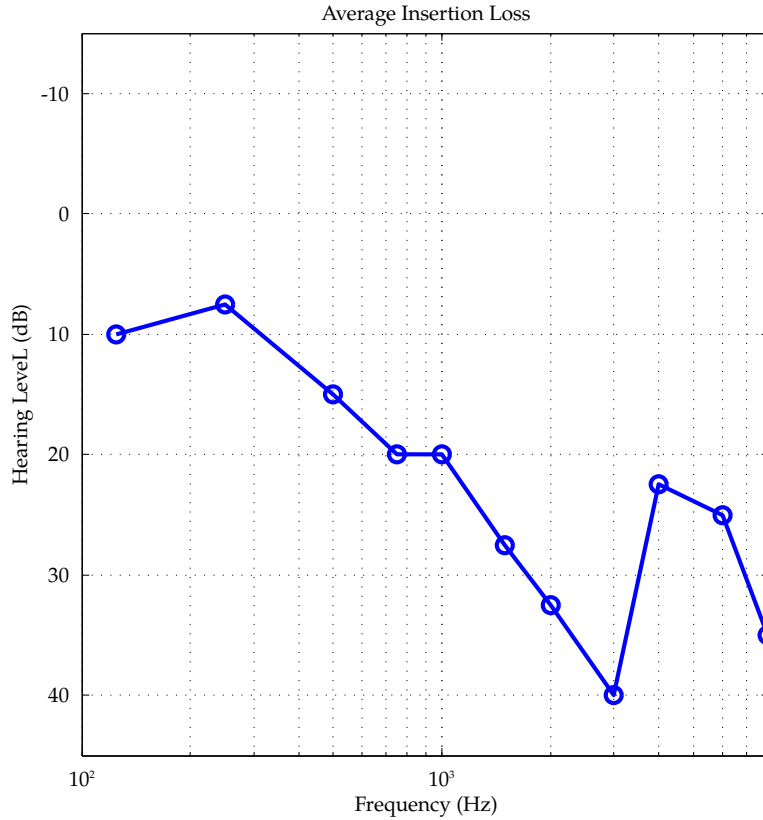
Figure 2.6: Insertion loss average as determined by measurements. Measurements available in appendix C.

Microphone Placement

The placement of the microphone is critical as it severely impacts the resulting HRTF's. The Microphone placement will define how close the response of the system can get to the natural response without the system. The characteristics related to the HRTF's should be altered as little as possible by the signal captured with the microphone. Extensive measurements are done in order to determine the optimal position of the microphone on the in-ear

headphone, for specific details on the measurements see appendix A.

There are several issues to take into account when placing the microphone. First it should be placed on the headphone in order to avoid the necessity of individualized headphone molds. Second is the space around the microphone, obviously it must not be blocked by any parts of the pinna. Third the HRTF's is assumed not to change much with relative small variations in placement of the headphone. This assumption is important, as any listener cannot be guaranteed to place the device identically each time.

Thirteen different microphone positions were evaluated, ten positions on the headphone and three positions on the ear(two in the concha, one on the tragus). The three placements on the ear were investigated to find if any advantage, that would justify the additional cost of an individualized headphone, is present. All the positions were compared to a blocked entrance reference measurement performed with the same microphone, and the difference between these were analyzed.

The two measurements conducted with the microphone placed in the concha show good results. These results are very similar to the $Azimut_{135}Attitude_{90}$ ($Azimuth_0$ is straight forward, $attitude_0$ is straight down) position with only small deviations for a few speaker directions. But as a position on the headphone showed similar results it was chosen instead. The measurements can be inspected in appendix A.
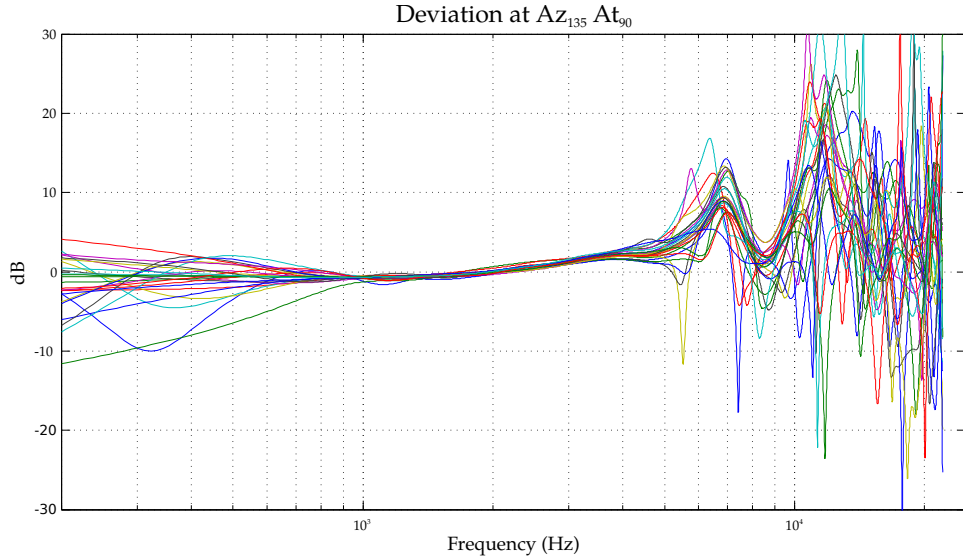

Figure 2.7: The HRTF difference between the blocked entrance reference and the measured HRTF at $Az_{135}At_{90}$.

Figure 2.7 shows the deviation for $Az_{135}At_{90}$. The ideal deviation is zero, but any deviation that is common between all speakers(directional independent) can be easily equalized. The difference for the 25 directions

coincide up to 8k-9k Hz. Above 10 kHz all directions vary independently. The difference in the low frequency area is not analyzed as the measurement system is unable to adequately reproduce frequencies in this part of the response.

Variation Of Head-Related Transfer Functions

A small study is conducted to examine the variation of the HRTF's from the artificial ear to a real human ear. The measurements are blocked entrance to secure low variation in microphone placement from subject to subject. The study is conducted on the assumption that the variation from the artificial ear to the subjects is small. This will allow measurements done in appendix A to be used as a measure for a general placement of the microphone. As long as the variation is within reasonable limits, the position chosen can be used for all listeners. Details on the measurements can be found in appendix B.

The subjects used are two females and three males in the age of 22-56 years of age. In figure 2.8 the blue line (subject 1) depicts the reference response measured with the artificial ear. The high pass effect is as in the previous measurement caused by the amplitude response of the speakers. The reference shows 3 significant notches for the frontal incidence(S_1). The general tendency of the reference measurement are in good correspondence with the ATF's of the measured subjects.

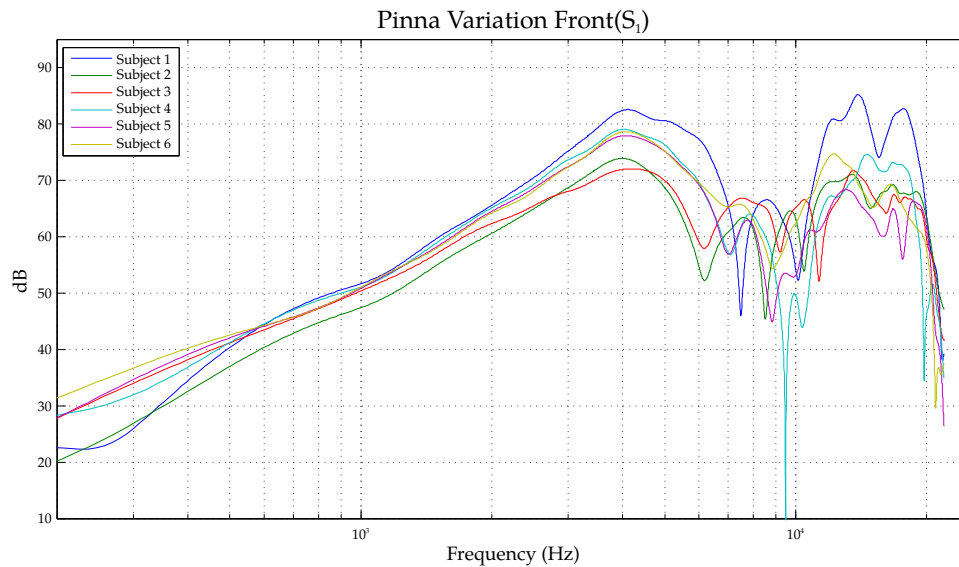

Figure 2.8: ATF of the 5 subjects, subject 1(blue) is the reference, front direction(S_1).

In table 2.1 the notches of the reference are compared to the variation of the notches of each subject. The notch of the reference is in all cases

very close to or within the variation of each subject. The higher the frequency the larger the variation of the subjects notches which can be due to the individuality of the pinna having a larger influence on the smaller wavelengths.

Front	1. notch	2. notch	3. notch
Reference	7.5k Hz	10.2k Hz	15.6k Hz
Variance	6.2k - 7.1k Hz	8.6k - 10.4k Hz	11.4k - 17.7k Hz

Table 2.1: Table of significant ATF features, reference and variations of subjects pinnae.

Besides the frontal incidence four other directions are examined these are: top (S_5), back (S_9), bottom (S_{13}), and side (S_{25}). The result of these can be seen in appendix B. The tendency is that the subjects ATF's in general follow the reference and hereby makes it possible to utilize the microphone position found with the artificial ear.

Chapter 3

Design

This chapter describe the design and development of the entire system. The first sections contain an overview of the system, describing the methods used to ensure system transparency. It furthermore describe the electrical signal path through the system and the influence of the different hardware elements. The next sections describe the development of equalizers for both microphone placement and headphone response focusing on the transparency of the system. After equalizing the implementation on the system platform is described. The next part is focused on the head tracking and implementation and HRTF filtering of the virtual signal. The last sections of the chapter describe the hardware design of the processing platform.

3.1 System Transparency

As mentioned throughout the previous chapters it is important to ensure transparency of the entire system. This requires that all hardware and software have no influence on the signal. As discovered in the preliminary studies 2.7 the insertion of the in-ear headphone and the placement of the microphone have an influence on the response of the microphone. In order to ensure transparency, any altered frequency response should be corrected with an inverse filter response to secure a resulting response with a zero dB passthrough for all frequencies. Beside the altered response at the microphone the headphone also has an influence on frequency response. The procedure applied for the microphone placement equalization is applied to the headphone swell. Besides the frequency response of the hear through device it is also important that the sound level is unaltered. For this part a calibration is done ensuring that the levels are the same.

3.1.1   Signal Path

Figure 3.1 shows the the signal through the system. Each element of the system contribute to the total signal path frequency response.

The first element is the microphone. The frequency response of a microphone is not entirely flat from 20 Hz to 20 kHz. The analog signal from a microphone is low voltage. Because of this low voltage value noise is easily induced in the signal, which is the main reason for the next element. The signal from the microphone has to be amplified before entering the processing platform. It is however important that the gain of the amplifier is equal for the entire spectrum of interest in order to secure transparency. The amplified analog signal has to be converted to a digital representation before the signal can be handled by the digital signal processor(DSP), this is done by an analog to digital converter(ADC). The main element is the DSP where all filtering is done. The DSP has two inputs one from the microphones and one from the virtual source. The two signals are merged together in the DSP and altered respectively. The merged signal is then converted back to analog by a digital to analog converter(DAC). The signal is then passed to a headphone amplifier which drives the headphone of choice, again it is important that the amplifier has no spectrum altering contribution to the signal. The final step is the headphone, this will inevitable have an influence on the spectrum of the signal which is played back and it has to be equalized.
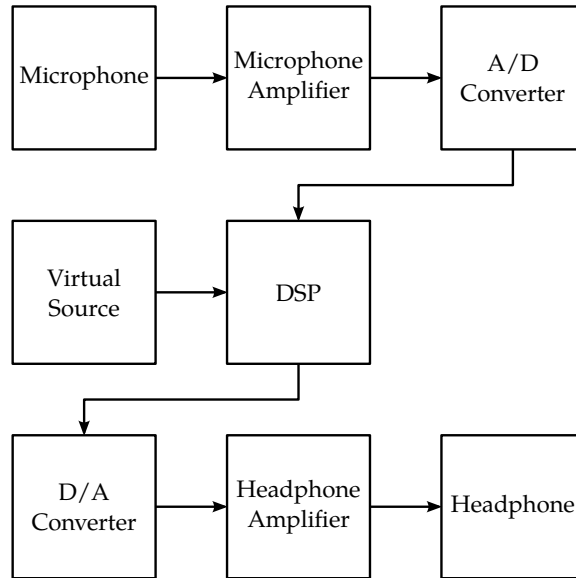

Figure 3.1: Electrical signal path.

As mentioned different elements in the signal part contributes to an alternation of the response and affects the transparency of the system. In figure 3.2 the signal path inside the DSP is shown. There are three sources

to handle, one from each microphone and one from the virtual input source. The signal from the microphones are first equalized with a filter that ensures that the artifacts from the placement of the microphone is removed. This filter is only applied too the microphone input. The virtual source has to be filtered with the HRTF's as a function of the position specified. The signals are then merged to their respective channels before a final equalizing takes place. This equalizing removes the response from the headphone. This conclude the signal path within the DSP.
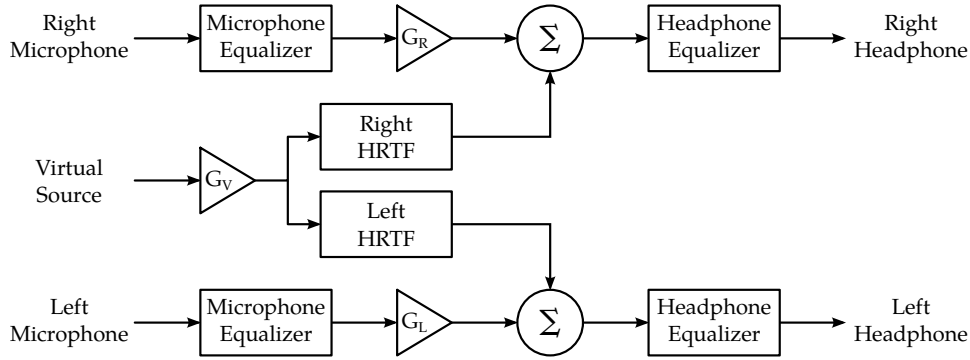

Figure 3.2: Filter signal path.

3.1.2 Microphone Placement Equalizer

In order to equalize for the the microphone position chosen, a filter with an inverse response has to be developed. As discovered in 2.7 the 25 different speaker directions frequency response coincide with each other up to ≈9 kHz. In order to equalize, the average response of all directions is found. This is done by taking the average difference of all 25 responses ending up with one frequency response. As mentioned the response above ≈9 kHz does not coincide for all directions. This implies that the equalizer should not alter the frequencies above ≈9 kHz. Furthermore as shown by the audiometry measurements the insertion loss at low frequencies is low. In view of this, alternation of the response at low frequencies is not advisable due to the transparency of the headphone. The response has to be shaped to fit with the above mentioned design parameters. The frequency response is shaped so the response below 1 kHz and above 9 kHz will go towards 0 dB alternation. The response is also normalized to 1 kHz, this is done to all filters in the signal path to secure an equal equalization throughout the system. In figure 3.3 the shaped frequency response is shown together with the chosen response from the 25 speakers at the microphone position. It is approximated with a 1500 coefficient finite impulse response(FIR) filter to secure high resolution of the frequency response. As seen in the figure the shaped response does not change abruptly to 0 dB alternation at 9 kHz, this secures a smooth

transition for the high frequencies so the alternation should be heard as little as possible.
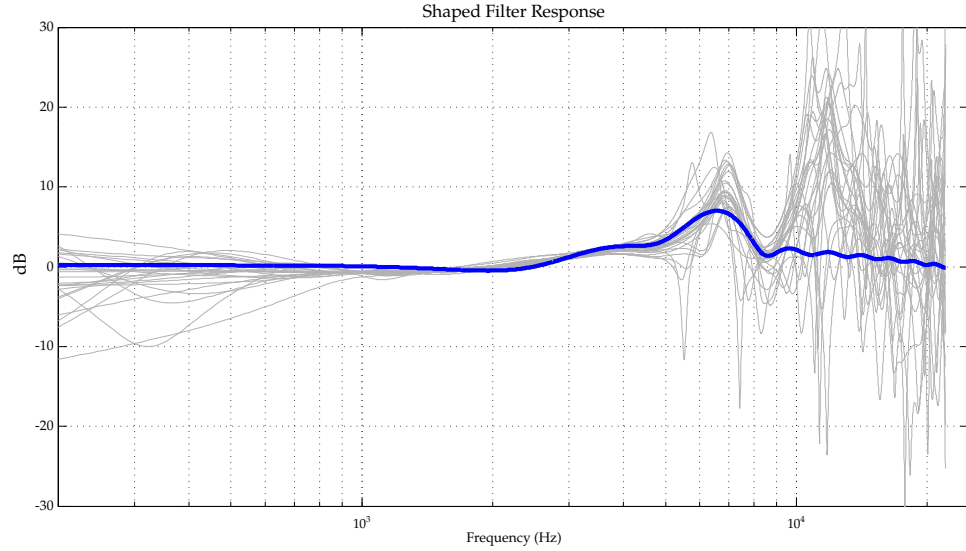

Figure 3.3: Shaped response of microphone placement filter approximated with 1500 coefficient FIR filter. Measured deviations show in in gray.

The shaped filter in figure 3.3 represents the response to be equalized, it is therefore necessary to invert the response in order to remove the altered response caused by the microphone placement. The shaped response is represented with an FIR filter. The properties of the FIR filter result in a pole located at zero but the zeros might be placed both in and outside of the unit circle with no effect to stability of the filter. But the zeros location affect the phase of the filter. For the filter to be fully invertible both with amplitude and phase response it is necessary to transform the filter to a minimum phase filter. This ensures that the filter has the same amplitude response with the zeros located inside the unit circle and that the filter is fully invertible.

In figure 3.4 the inverted response is shown. The response is generated with a 20 coefficients FIR filter which is sufficient. The criteria for sufficiency is that the resulting response is within $\pm$ 1 dB. The reason to decrease the amount of coefficients as much as possible is due to the implementation on the developed hardware. The hardware has a finite amount of operations within each sample and to avoid unnecessary use of computational time the FIR filters should remain as short as possible.
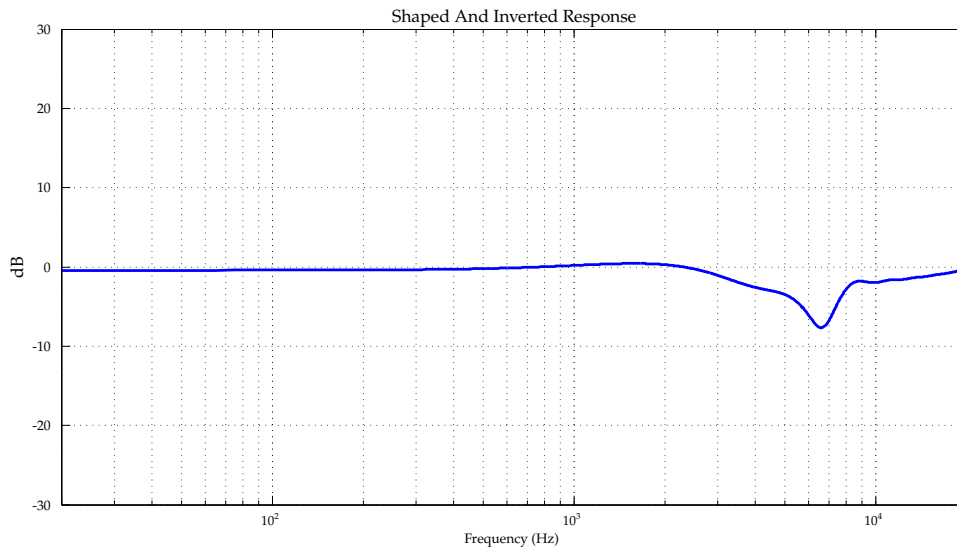
Figure 3.4: Inverted and shaped frequency response, approximated with 20 coefficient FIR filter.

The main goal of the equalizer is to create a flat response when applied to the signal acquired by the microphone. This results in a close approximation of a blocked entrance measurement which contains the spatial information. The theoretical resulting response after equalizing can be viewed in figure 3.5. Some ripple is observed at the passband of the filter. This is due to the approximation with a short FIR filter. The ripple is within $\pm$ 0.6 dB which is expected to be inaudible for any listener.
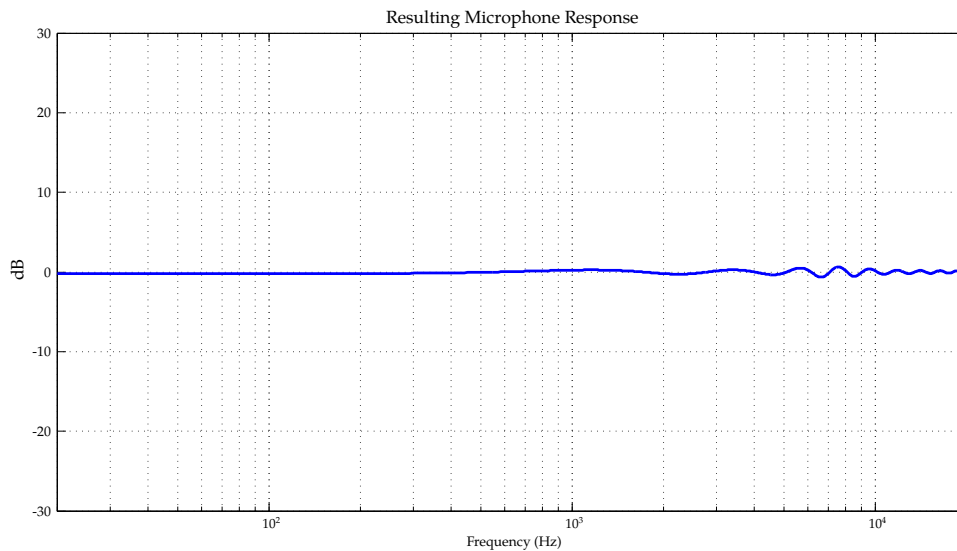

Figure 3.5: Resulting response after equalizing the microphone placement.

The filter is as mentioned earlier only applied to the input from the micro-
phones, and will have no influence on the virtual part of the system. The
MATLAB code to generate the figures and calculate the filter coefficients is
located at ⊙/Matlab/Microphoneplacementfilter/ver2_eq_mic.m

3.1.3   Headphone Equalizer

The in-ear headphone used is the last hardware element in the system before
the sound arrives at the eardrum. The ideal headphone would have a flat
frequency response across the entire spectrum. However as found in D the
response of the headphone is not flat. This will inevitably affect the trans-
parency of the system. Only one channel of the headphone is measured as it
is assumed that they do not differ significantly. As with the microphone it is
possible to derive an equalizer securing a flat response from the headphones.

In figure 3.6 the shaped response of the headphone is shown. The re-
sponse is normalized to 1 kHz which is used as a reference point for the
equalizing filters. As seen in the original response of the headphone (figure
D.1 in appendix D) the response has a significant roll off at the lower and
upper end of the spectrum. If care is not taken the equalizing filter will have
to amplify excessively at both ends. This can result in overdriving the head-
phones causing distortion of the sound. To avoid this behavior appropriate
cutoff frequencies are chosen. The frequencies chosen are 50 Hz for low-cut
and 11 kHz for high-cut. The response is shaped to go towards 0 dB for all
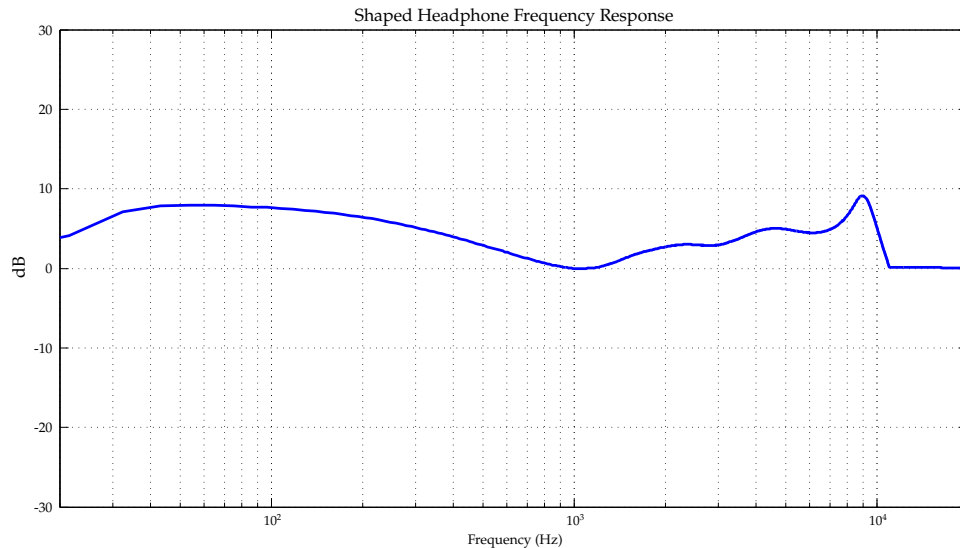frequencies outside the chosen passband.

Figure 3.6: Shaped frequency response of AKG K323XS headphone.

The headphone response is derived from the impulse response obtained in the
measuremtns. The response consist 65535 samples. That is however to many

coefficients to handle on the processing platform. Again the response has to be inverted for it to equalize the affects of the headphone. The minimum phase transform is applied to secure full invertibility of the response. The inverted response is seen in figure 3.7, the response is approximated with a 30 coefficient FIR filter.
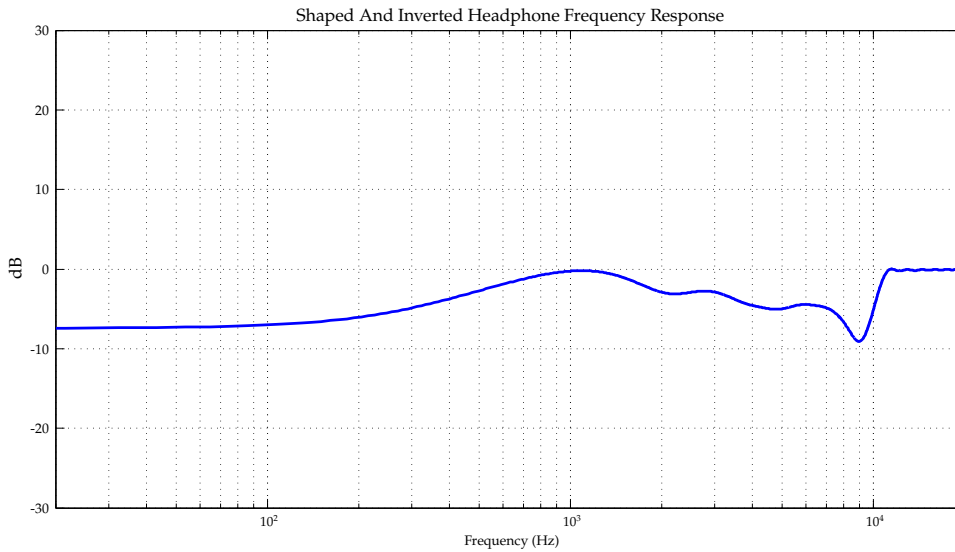

Figure 3.7: Inverted shaped frequency response, approximated with 30 coefficient FIR filter .

The theoretical resulting response can be seen in figure 3.8. The response in the domain above 200 Hz has some ripple, but it is less than $\pm$ 1 dB, which is acceptable. The domain below 200 Hz has some gain which is introduced due to the short length of the FIR filter. To avoid the effects below 200 Hz the length of the FIR filter would increase significantly and thereby use valuable processing time on the DSP.

This filter will apply to all signals in the system as the headphones serves as the last element in the signal path. The MATLAB code to generate the figures and calculate the filter coefficients is located at `/Matlab/Headphone_eq/headphone_eq.m`.
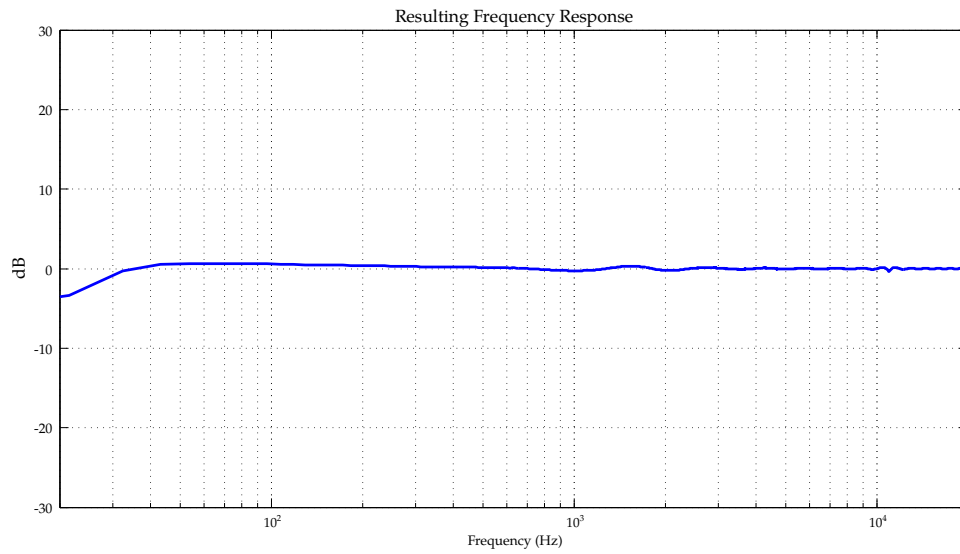
Figure 3.8: Resulting response after equalizing the AKG k323XS headphone.

3.1.4   Equalizer From Microphone To Headphone

The filters designed in the previous sections will together be the entire equalizing from microphone input to headphone output. As mentioned transparency is of great importance as this will ensure a natural. The equalizing of both elements yield the theoretical resulting response shown in figure 3.9.

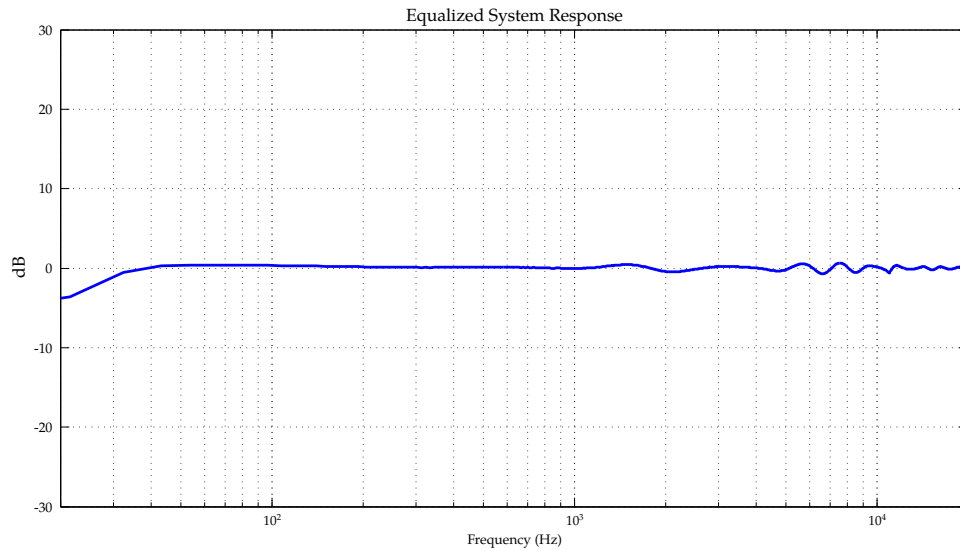**Figure 3.9:** Resulting response after equalizing the system from microphone to headphone.

As seen the equalizing of the headphone has the most influence on the

resulting response. It should be noted that this response does not apply to the virtual signal path.

3.1.5 Calibration

The signal path from the microphones to the headphone goes through several hardware elements. These elements also contributes to the amplitude of the signal, especially the amplification in the microphone amplifier. And as a result the amplification in the microphone amplifier may not always fit the microphone used. In view of this a calibration of the entire system from microphone to headphone is needed to secure full transparency of the system. A 94 dB input should yield a 94 dB output from the headphone. Due to the normalization of the equalizing filters at 1 kHz it is possible to calibrate at this frequency with a know input. The calibration should be done every time a change to the hardware is done. It is possible to adjust the level of the output either when the signal enters the DSP or in the DAC if it features any kind of volume control.

3.2 System

The system is comprised of two parts. The first part includes the hear through device and the second part is the processing platform. The basic idea is to keep the platform as open as possible, in order to serve as a development tool for future device investigation. In figure 3.10 the proposed enclosure of the system is seen. The case is intended to be small for wearability and is small enough to fit in either a belt clip or pocket. A closer look at the enclosure in figure 3.11, reveals the user interface. In order to show system setup and give the user the ability to do configuration, a display and a scroll contact with a push button is placed at the top. The connections shown on the enclosure connect to each hear through device (left and right). The connectors should contain all connections necessary to service the hear through device. The 3D drawing is realized with OpenScad and can be viewed at ⬤`/Hardware/case.scad`.

The processing platform will process the microphone signal, handle the directional information and process a virtual source accordingly. The microphone signal will to be equalized as discussed in 3.1.2. Handling the inputs and virtual source also requires mixing. The headphone also requires equalization as discussed 3.1.3. The power is supplied from a battery as the entire system is wearable, and free of any cords except the connections between the hear through device and processing platform.

Figure 3.10: Proposed enclosure containing processing platform.
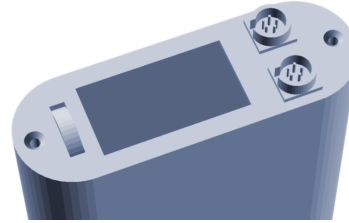
Figure 3.11: Close up of proposed user interface, with display, connectors and scroll switch.

The hear through device must be small and light as it will be fitted at the ears. Apart from the microphones and headphone, information regarding the direction of the listeners head is also collected by the device. It is important for the application that the device closely matches orientation of the head when fitted, in order to keep a steady virtual source direction matching the actual orientation.

Figure 3.12: Block diagram of the system, illustrating the elements of the system.

Figure 3.12 illustrates the elements of the total system including hear through device and processing platform, each of the blocks represent a module. The dotted line delimits the interface between the hear through device and pro-

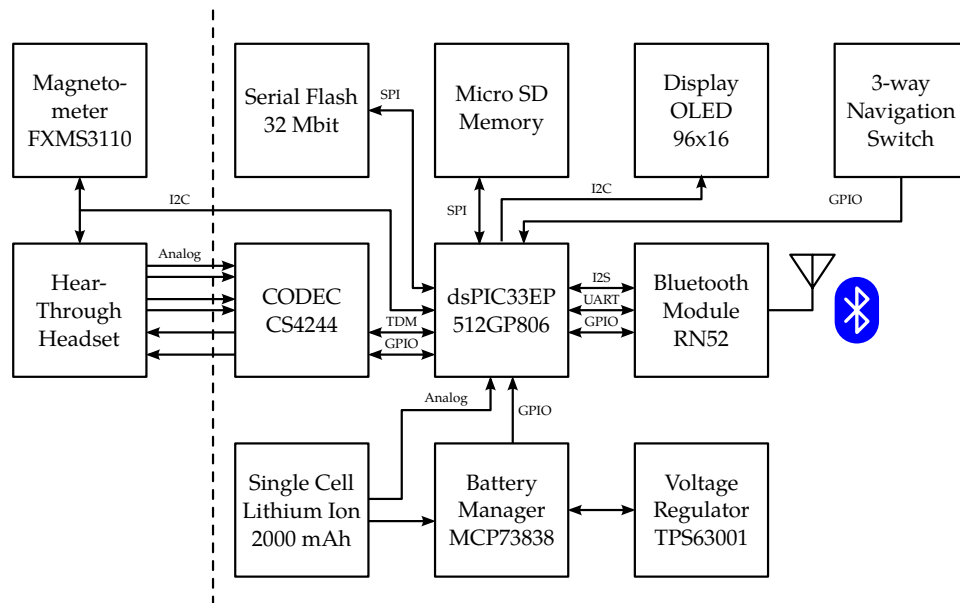cessing platform. In the following sections the design of the hardware is specified for each of the main modules in the block diagram on figure 3.12. The electrical characteristics of the system are documented in appendix E.3. A brief system manual is available in appendix E.

3.3 Interfaces

Several interfaces are handled internally and externally. The external interfaces must allow for several hear through device configurations. This is achieved by presenting four analog channels in and out of the processing platform combined with a private I2C digital bus. Two of the analog output channels are optionally buffered through a headphone driver. This interface allows large variations in the hear through devices. The I2C bus allows several digital devices to communicate with the processing platform. Refer to appendix E.8 for complete hear through device electrical connection.

The implemented hear through device utilizes an electronic three axis compass to determine head orientation. The sensor is an FXMS3110 (datasheet found at `/Hardware/OrientationSensor/`), and interfaces via an I2C bus. The sensor allows sampling at up to 80 Hz with a one degree accuracy. The advantage of a compass is the fixed orientation (magnetic north). An accelerometer only samples acceleration and the head orientation must be derived from this, resulting in drift over time where the compass always reads the magnitude of the earths magnetic field in three orthogonal directions. This reading allows an absolute heading to be calculated at every sample.

The virtual source can originate from several depending application needs. The intended source is a wireless connection but the analog input channels could also be used for real time sources. The addition of on-board mass storage allows for prerecorded signals to be played back on demand. The wireless connection is realized via a Bluetooth connection, this allows easy access form many devices and supports real time stereo playback. As the Bluetooth software stack and RF transceivers would complicate the system development considerably a "Bluetooth-in-a-box" solution is realized in the RN-52 device from Microchip `/Hardware/Bluetooth/RN-52/rn-52-ds-1.1r.pdf`. The RN-52 is a self contained device and handles everything concerning the Bluetooth stack (discovery, pairing and so on). It supports several protocols of which only A2DP(Advanced Audio Distribution Profile) and SPP(Serial Port Profile) is required. The device is configured using the UART connection in conjunction with a GPIO to signal command mode. The RN-52's audio interface is configured to interface via I2S transmitting a PCM signal. The module only generates a sample rate signal when audio is transmitted and it depends on the source sample rate. Because of this it is not feasible to synchronize the module and system as the processing

platform must be locked to 44100 Hz at all times. Transmitting anything else will result in artifacts if the signal is not re-sampled. The RN-52 allows the audio interface and serial port simultaneously. This grants an interfacing device the ability to communicate with the processing platform as well as stream audio. Refer to appendix E.8 for complete Bluetooth electrical connection.

The user interface is comprised of a 16x96 pixel OLED display connected to the internal I2C bus. An OLED display was chosen for the very high contrast ratio. The display is a monochrome pixel matrix allowing graphics to be displayed. An OLED display is very energy efficient as it requires no backlight, only the pixels that are on require power. OLED's are common in the small sizes required by the enclosure. The display has an on-board interface controller which handles the display and voltages. The device datasheet can be viewed at ⊚`/Hardware/Datasheets/Interface/MCOT096016AV-WI.pdf`.

The user input is a center push momentary clockwise and anti clockwise lever. This configuration requires three buttons to be monitored for user input. The device datasheet can be viewed at ⊚`/Hardware/Datasheets/Interface/MCPL3-BC-V.pdf`.

3.4 CODEC

The processing platform is built around the CODEC. A four channel device is chosen as the project proposal also introduces the possibility of using several microphones to cover a wider dynamic range. Very few actual multichannel devices are available, most employ multiplexing schemes and only contain one or two converters. Multiplexing converters usually results in a performance degradation. Two stereo CODEC's could be used, but would increase the system complexity unnecessarily. Cirrus Logic produce an actual four channel CODEC in a small package with good specifications. The CS4244 is a 4 channel 24 bit converter, the datasheet is available at ⊚`/Hardware/CODEC/CS4244.pdf`. The converter accepts a differential input biased around half supply and requires only a few passive components for decoupling. The converter is configured from an asynchronous I2C bus. This control interface is connected to the processing platforms internal I2C control bus. The connections of the CODEC can be seen in figure 3.13.
The CS4244 can be operated from a single supply, but is not in this design to improve performance. The digital interface is operated from the digital supply and the analog interfaces are powered from the analog supply. The CS4244 employs a ramp on power up resulting in no transients from the DAC when powering on or off.

The DSP interface to the CODEC can be realized as two independent stereo converters with separate I2S Left Justified data in/out paths. The
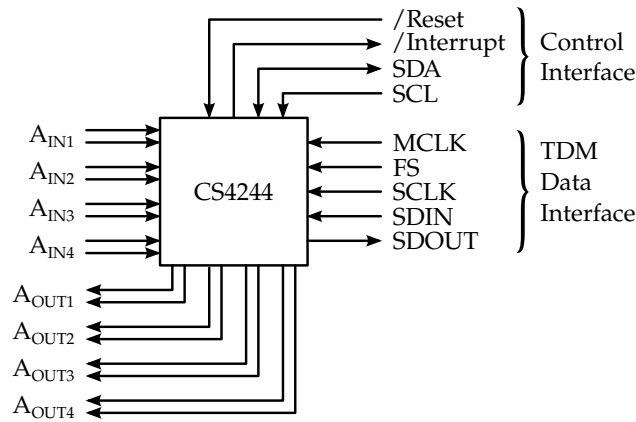
Figure 3.13: CODEC digital and analog interfaces overview. See appendix E.8 for schematics.

second option is a single TDM (Time Division Multiplexed) interface. This interface is chosen because it allows the DSP to be interfaced using only a single port (up to four CS4244 devices can be interfaced through this bus). The TDM interface requires the SCLK frequency to be 256x or 512x Fs.
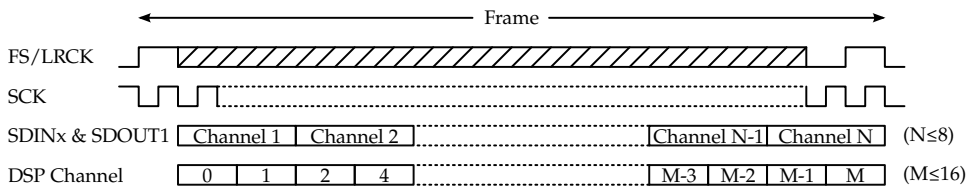

Figure 3.14: CODEC TDM frame overview.

The CODEC TDM frame format is 32 bit but the DSP can only handle 16 bit frames (see figure 3.14). This is not a problem as the DSP can still read all of the bits in the TDM frame, but handles them as 16 bit words instead. This means that the eight frame TDM is handled as a sixteen frame TDM in the DSP resulting in the most significant word in even channels (0,2,4,6) and the remaining byte in the following odd channel. As the DSP is only 16 bit the last byte is discarded.

3.5 Microphones

The system is intended as a research platform and to this end the microphone choice is largely ambiguous. But for demonstration purposes a microphone is implemented. Several microphones are investigated, all are MEMS (Microelectromechanical systems) type microphones. This type of microphone is chosen as it is very small, allowing mounting on the in-ear headphone, and still offers reasonable performance. None of the microphones offer a dynamic

range to match human hearing, so any choice is a compromise.

A brief overview of the investigation is shown in table 3.1. One of the critical features is the SNR(Signal to Noise Ratio). This is the point of comparison because it is desired to cover as wide a dynamic range as well as possible with a single microphone.

Brand	Part	SNR	Bandwidth	Price
Wolfson	WM7121	65 dB$_A$	62-15k Hz	2.00 \$
Wolfson	WM7131	65 dB$_A$	85-12k Hz	1.74 \$
Knowles[†]	SPM0408LE5H	63 dB$_A$	100-10k Hz	4.00 \$
Analog Devices	ADMP504	65 dB$_A$	100-20k Hz	3.60 \$
Analog Devices	ADMP803	67 dB$_A$	80-20k Hz	20.00 \$
ST	MP33AB01H	66 dB$_A$	100-10k Hz	2.50 \$

Table 3.1: List of microphones of interest. † Amplifies the signal 20 dB. Equivalent input noise is 29 dBA if stated by datasheets. Prices are single quantity price.

It should be noted that the microphones with a wide frequency range have a peak at approximately 10 kHz probably caused by an internal filter compensation. Price is usually indicative of performance in electronics, unfortunately it is not linearly dependent as can clearly be found in the table above. The frequency range has to be wide considering the applications of this project.

Based on the investigation the WM7121 was chosen. Unfortunately it was impossible to acquire so an alternative is used instead. The WM7120A is a very similar device with lower performance, and it is already used in measurements performed in appendix A and B. The WM7121 can replace the WM7120A, as the electrical interface is the same, and improve the overall system performance.

3.6   Microphone Amplifier

The microphone needs amplification to make the most of the CODEC's electrical interface. This amplification should be close to the microphone to minimize noise induced in cabling. The orientation sensor already requires electronics fitted to the users head, so locating the amplifier here is an obvious choice. The amplifier must amplify the signal from the microphone sufficiently and should ideally be included in the microphone. But no microphone offers an output that matches the CODEC interface. The WM7120A has a sensitivity of 42 dBV at 94 dB, resulting in 42 dBV $= 10^{\frac{-42 \text{ dBV}}{20}} = 7.9$ mV$_{\text{RMS}}$. A sound level of 106 dB is chosen as the maximum level resulting in an equivalent 12 dB voltage gain. The resulting maximum expected voltage from the microphone is then $10^{\frac{12 \text{ dB}}{20}} \cdot 10^{\frac{-42 \text{ dBV}}{20}} = 31.6$ mV$_{\text{RMS}}$. From this voltage an amplifier gain can be determined by solving:

$$2\sqrt{2}\left(10^{\frac{A_{\text{mic}} \text{ dB}}{20}} \cdot 10^{\frac{12 \text{ dB}}{20}} \cdot 10^{\frac{-42 \text{ dBV}}{20}}\right) \tag{3.1}$$

The CODEC does not accept differential voltages above $\frac{1}{2}(1.58 \cdot V_A) = \frac{1}{2}(1.58 \text{ V} \cdot 3.3 \text{ V}) = 2.607 \text{ V}_{\text{pp}}$. Keeping this in mind an A_{mic} of 28 was determined. Resulting in a maximum voltage presented to the CODEC of:

$$2\sqrt{2}\left(10^{\frac{28 \text{ dB}}{20}} \cdot 10^{\frac{12 \text{ dB}}{20}} \cdot 10^{\frac{-42 \text{ dBV}}{20}}\right) = 2.247 \text{ V}_{\text{pp}} \tag{3.2}$$

Leaving $\frac{1}{2}(3.3 \text{ V} - 2.247 \text{ V}_{\text{pp}}) = 0.527 \text{ V}_{\text{p}}$ margin for the amplifier but only $\frac{1}{2}(2.607 \text{ V}_{\text{pp}} \text{ V} - 2.247 \text{ V}_{\text{pp}}) = 0.180 \text{ V}_{\text{p}}$ for the CODEC.
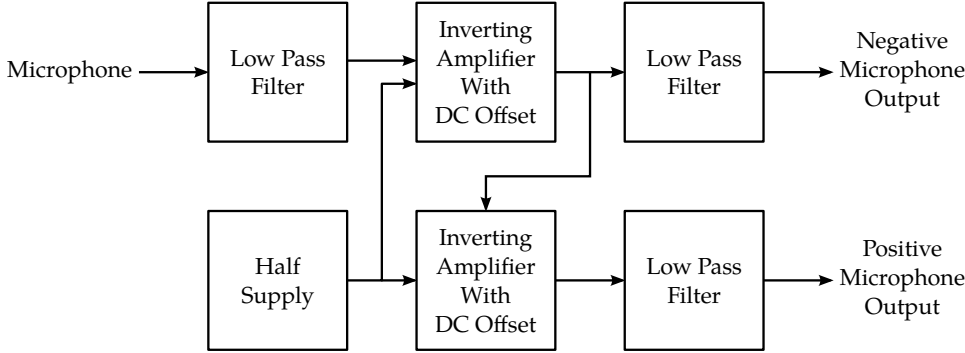

Figure 3.15: Microphone amplifier block diagram. See appendix E.8 for schematics.

The block diagram in figure 3.15 illustrates the amplifier structure. The DC offset from the microphone is 0.6 V (allowing 0.6 V swing at the minimum 1.2 V supply). The microphone input is fed through a DC blocking RC filter to remove this offset before the signal is amplified.

The amplification is achieved through dual operational amplifier (single package). The first amplifier amplifies the signal 28 dB around a half supply offset of 1.65 V. It is bandwidth limited to decrease noise as noise is a function of bandwidth. The amplified signal is buffered and inverted by the second stage, resulting in two signals of equal magnitude centered at half supply 180 degrees out of phase. The differential signal results in a gain of 6 dB when it is summed again. Simulations of the idealized model can be found in ⊙/Hardware/LTSPICE/. In a transient simulation a small offset of approximately 100 mV is observed. If the output offset is identical the op-amps will offset equally in opposite directions and the offsets will cancel each other. This behavior should translate to the real op-amps, as dual package devices tend to perform equally.

The outputs are fed through anti-aliasing low-pass filters before they are sent to the cable connecting them to the CODEC. The capacitors in this filter

are relatively large to allow smaller series resistance resulting in a smaller overall signal voltage loss.

The op-amps were chosen based on several criteria, first and foremost small package size as it will be fitted close to the ear. Electrically the op-amps should operate at single supply voltage of 3.3 V supplied by the system. Rail-to-rail operation is preferred to utilize the full range of the CODEC and improve signal integrity. Lastly the amplifier linearity must be ensured. It must have sufficiently high gain bandwidth product to amplify within the desired bandwidth, and low noise. Based on these criteria the TS972 is chosen, it can be viewed in greater detail in the datasheet found at ⊙/Hardware/Datasheets/CODEC/.

3.7   Headphone Amplifier

To allow the system to interface most headphone types an amplifier is needed to drive the headphone and convert the differential signal from the CODEC into a single ended headphone level signal.
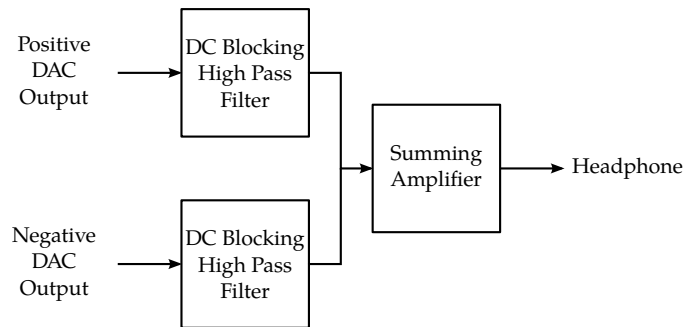

Figure 3.16: Headphone amplifier block diagram, one channel shown. Amplifier generates negative voltage from supply internally to achieve line level voltage swing. See appendix E.8 for schematics.

Using the TS972 op-amp to buffer and sum the differential signals can be realized to simplify design. The system supply voltage unfortunately does not allow for a full *line* level voltage swing. The supply voltage is simply not great enough. The only solution is to generate the required voltage. To keep it simple and not change the power supply, an integrated solution is used. The MAX97220A is a differential input line driver/headphone amplifier(see figure 3.16). It is capable of driving 2 V_{RMS} into 600Ω loads from a 3.3 V supply, has a *"Flat THD+N, Better Than 90dB in the Audio Band* and *109dB SNR when powered from 3.3 V"*. Datasheet can be viewed at ⊙/Hardware/COEDC/MAX97220A.pdf. It generates a bipolar supply by generating an inverse supply voltage with an on board charge pump. The output is then biased around 0 V and the driver is intended to be directly

coupled to the load. The inputs are fed from the CODEC through a DC blocking high pass filter, to allow the driver to self bias optimally. Inherent in the differential to single ended amplifier is a 6 dB signal gain as mentioned in 3.6. The resulting total system gain is then 34 dB as the CODEC does not contribute. The device is internally bandwidth limited but the board layout allows adding additional bandwidth limiting by adding capacitors in the feedback.

3.8 Digital Signal Processor

The choice of DSP is mostly application requirement specific. As the hear through application requires only modest processing power, very large scale multi core DSP's are not considered. To simplify implementation Microchips dsPIC range of *Digital Signal Controllers* are investigated. These devices are very similar to micro controllers in every respect, except for the efficient DSP instruction core. The dsPIC33E is a 16 bit fixed point Harvard structure, MIPS derivative register based DSP capable of up to 70 MIPS and is available in several memory configurations. Because the processing platform is not specifically targeted at a single application the largest device was chosen to allow very large applications. This device has 512 KB program memory and 52 KB RAM. The micro controller parallels in the DSP results in very flexible pin remapping of internal peripherals. The deciding factor in choosing the dsPIC is the very good free cross platform compiler and IDE.

3.8.1 Clock

Clocking is an integral part of any digital sampling system. To ensure predictable operation the DSP clock is closely fixed to the sample rate. This ensures a fixed amount of instructions performed between each sample. As the CODEC requires the interfacing DSP to be the master device when driven in the TDM mode several clocks must be generated by the DSP. The DSP interfaces the CODEC via the DCI(Data Converter Interface) peripheral. This peripheral allows hardware control and decoding of the TDM stream. The DCI is not able to generate the MCLK required by the CODEC. This poses several difficulties as this clock is required and must be synchronous with the TDM signals. The DCI is driven from the internal instruction clock, and because of this the main clock can be used as the MCLK. This however requires the DSP to generate its instruction clock from the MCLK.
Figure 3.17 illustrates the internal clock distribution in the DSP. The DSP has an internal reference clock buffer (and divider) which can be remapped to an output pin. This buffer is utilized to serve as the CODEC MCLK. Because the DSP has an internal PLL, it is able to generate its instruction clock from several input frequencies. Recall from section 3.4 that a clock
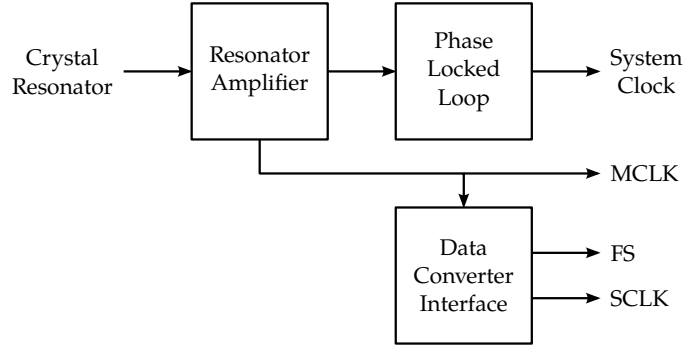
Figure 3.17: Block diagram of clock generation and distribution. All peripherals are driven from the system clock. See appendix E.8 for schematics.

of 22.5792 MHz is required(CODEC MCLK). This clock will be used as a reference clock to generate all internal clocks including the instruction clock.

Figure 3.18 illustrates the PLL structure which is utilized to generate the DSP instruction clock. All information regarding the DSP's internal clock system can be found at ☉`/Hardware/DSP/Section7.Oscillator.pdf`.
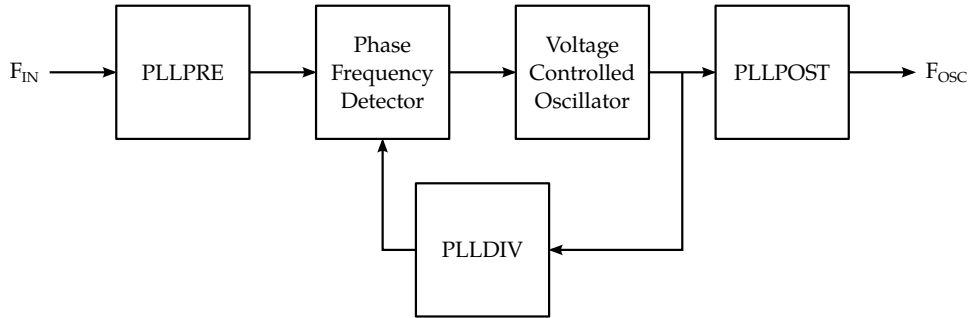

Figure 3.18: Simplified Phase Locked Loop figure 7-8 from ☉`/Hardware/DSP/Section7.Oscillator.pdf`.

The instruction clock realized from the PLL is derived using the following expression:

$$F_{OSC} = F_{IN} \cdot \left(\frac{PLLDIV + 2}{(PLLPRE + 2) \cdot 2(PLLPOST + 2)} \right) \tag{3.3}$$

The expression has several limitations. First F_{IN} must be configured to allow one of the following modes:

- HS Crystal Oscillator mode (10 MHz to 60 MHz)
- XT Crystal Oscillator mode (3.5 MHz to 10 MHz)
- EC (External Clock) mode (0 MHz to 60 MHz)

Second compliance with several internal limits must be ensured:

- Phase Frequency Detector input 0.8-8.0 Mhz
- PLLDIV 120-340 MHz
- F_{OSC} 0-140 MHz

Thirdly the range of each block limits the possibilities:

- PLLDIV $[2, 3, ..., 513]$
- PLLPRE $[2, 3, ..., 33]$
- PLLPOST $[8, 4, 2]$

The first condition is already determined by the crystal choice as determined by CODEC MCLK requirement. The remaining conditions are realized using a small program to iterate every possible configuration and find the optimum performance. The program is written in Python and can be viewed at ⦿`/Software/fosc.py`. The result is: PLLPRE = 3, PLLDIV = 36 and PLLPOST = 2 resulting in a 135.4752 MHz operating frequency. The DSP's instruction clock is $F_{CY} = \frac{F_{OSC}}{2} = \frac{135.4752 \text{ MHz}}{2} = 67.7375$ MIPS. At this clock 96% of the DSP's rated speed is achieved resulting in $\frac{67.7375 \text{ MIPS}}{44100 \text{ kHz}} = 1536$ instructions per sample.

A two speed startup is required by the DSP to ensure the PLL has stabilized before switching the clock source. The internal RC oscillator is used as a fall back should the main PLL fail.

3.9 External Memory

Two external memories are present on the system. The primary external memory is the serial flash. A serial memory is chosen to simplify board layout. The memory is intended to store the HRTF database and should have a size that allows for this. High density high speed serial flash is very common and very cheap. The drawback of flash memory is the inability to overwrite data. It must first be reset (to 0xFF) before it can be written, and this is usually only possible in 4k byte sectors or more. It should not pose any problems as the flash will only serve as storage and only be written if the complete filter database is changed. The Valdemar HRTF database is just below 12 thousand HRTF sets [Christensen., 2000]. Approximated memory requirement to store the entire database in 16 bit, 80 coefficients which should be sufficient is [Blauert, 2005]:

$$2 \cdot 12 \cdot 10^3 \cdot 2 \, \frac{\text{Byte}}{\text{Coeffecients}} \cdot 80 \text{ Coeffecients} = 3.84 \text{ MB} \tag{3.4}$$

A 32 Mbit (4 MB) memory is required based on the above calculation. An SST25VF032B Microchip device was chosen based on the calculation

in equation 3.4, the datasheet is available at ☺/Hardware/Other/. The
SST25VF032B is a 32 Mbit (4 MB) device and can be doubled to 64 Mbit
by substituting with a SST25VF064C. Speed is also a primary concern as
the memory is accessed randomly at high speeds. The SST25VF032B has
an 80 MHz SPI interface, resulting in a maximum transfer speed of:

$$\frac{80 \text{ MHz}}{8 \text{ bits/Byte}} = 10 \ \frac{\text{MB}}{\text{s}} \tag{3.5}$$

Initiating a continuous read requires only a single byte of overhead and is
therefore ignored. The time to transfer a complete filter set can then be
calculated:

$$\frac{10 \ \frac{\text{MB}}{\text{s}}}{4 \text{ Byte} \cdot 80 \text{ coeffecients}} = 500 \cdot 10^3 \ \frac{\text{Filter sets}}{\text{s}} \tag{3.6}$$

Unfortunately the SPI interface in the DSP cannot achieve these speeds and
is forced to settle for much more modest speed. The DSP can handle 9 MHz
full duplex and 15 Mhz simplex. Adjusting for the lowest speed the expected
speed is:

$$\frac{9 \text{ MHz}}{8 \text{ bits/Byte}} = 1.125 \ \frac{\text{MB}}{\text{s}} \tag{3.7}$$

$$\tag{3.8}$$

$$\frac{1.125 \ \frac{\text{MB}}{\text{s}}}{4 \text{ Byte} \cdot 80 \text{ coeffecients}} = 3515.625 \ \frac{\text{Filter sets}}{\text{s}} \tag{3.9}$$

The theoretical delay from direction change to new filter ready is then
$(3515.625 \ \frac{\text{Filter sets}}{\text{s}})^{-1} = 284 \ \mu\text{s}$. This speed is still sufficient to keep up
with the directional update speed assuming no overhead.

An SD card interface is realized using the low level SPI mode of the SD
card specification. The electrical connection can be found appendix E.8.
This allows for very large scale (128GB) memory to be installed. The SD
card interface is added to make the most of the platform and is not utilized
in this project. It does however allow for any use case that requires very
large amounts of data.

3.10   Power supply

Several defining characteristics of any electronics system design are a direct
result of power supply design. To this end some critical points must be
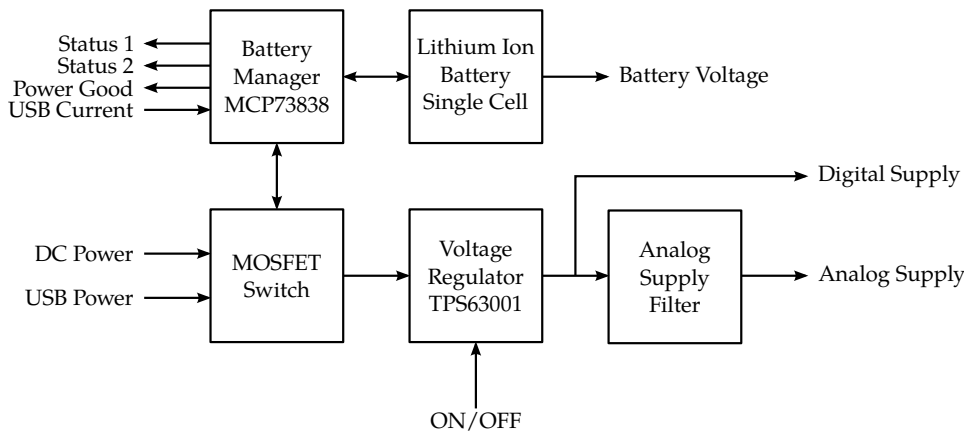considered in its design. The following sections concern the power supply

Figure 3.19: Block diagram of the power supply and battery system. Schematic is available in appendix E.8

design and considerations of the processing platform. Figure 3.19 illustrates the power supply system.

In order to minimize cost and complexity of the design, a single supply is chosen. Many digital parts are available with very low voltage requirements, but this leaves very little room for analog signals, which operate at higher voltages to suppress the noise floor. The trade off from higher supply voltage is increased power consumption, so a compromise is found. The processing platform is scoped to run at 3.3 V as most common digital parts are available at this voltage and it leaves sufficient room for analog voltage swing. This voltage does however mean that a full analog *line* level (2 V_{RMS}) cannot be driven from the supply.

3.10.1 Battery

For any portable system the battery is a defining characteristic. Battery voltage and capacity must be chosen carefully to meet the requirements of the system. Many battery types are available and based on the chemistry, they offer different characteristics. For a portable system size and weight is important and is also to be considered. The main battery concern is capacity, as it determines the operating time of the system. An estimate of the system power consumption is found in the following table:

Function	Device	Power
DSP	dsPIC33EP512GP806	105 mA
Display	MCOT096016AV	153 mA
Serial Flash	SST25VF032B	30 mA
Bluetooth	RN52	30 mA
Battery manager	MCP73837	<1 mA
Magnetometer	FXMS3110	<1 mA
Voltage regulator	TPS63001†	<1 mA
CODEC	CS4244	72 mA
Microphone	WM7120A	<1 mA
Amplifier	TS972	$2 \cdot 3$ mA = 6 mA
Headphone driver	MAX97220A	7 mA
Headphone(16 Ω)	AKG K323XS‡	$2 \cdot \sqrt{\frac{110 \text{ mW}}{16 \text{ }\Omega}}$ = 166 mA
Total		**577 mA**

†*Efficiency of the buck-boost regulator changes with load current and battery voltage.*

‡*Maximum output power from headphone amplifier in 16 Ω, AKG headphone rated at 10 mW!*

It is important to note that this figure is a very rough estimate and an actual characterization of the system must be done to know the exact load. All values are as close to the expected maximum load at 3.3 V as determined by the respective data sheets. Most devices change their power requirement depending on the task performed.

The system power consumption if found from the estimated total current to be $P_{\text{sys}} = U_{\text{sys}} \cdot I_{\text{tot}} = 3.3$ V $\cdot 0.577$ A = 1.904 W.

From the system power requirement it is apparent that a rechargeable battery is preferable. Four hours is the estimated maximum use case, this time should allow most possible applications to be run within one charge cycle. The battery must have a capacity of 4 h $\cdot$ 1.904 W = 7.616 Wh to allow this application time. Lithium batteries offer high capacities in small packages and are very popular in portable applications because of this. From available lithium batteries a 2 Ah single cell lithium ion battery is found. This battery yields an estimated $\frac{3.7 \text{ V} \cdot 2 \text{ Ah}}{1.904 \text{ w}} = 3.88$ h ≈ 3 h 53 min run time. The battery can be viewed in more detail at ☺/Hardware/Powersupply/ Battery.pdf.

The Characteristics of Rechargeable Batteries.pdf document by National Semiconductor contain discussions on specific characteristics of lithium ion batteries and is found at ☺/Hardware/Datasheets/PowerSupply/.

3.10.2   Battery Management

Lithium ion batteries are delicate things, and care must be taken to avoid *"...vent with flame"* and *"...spontaneous deconstruction"*. Luckily this battery type is very common and several off-the-shelf battery managers are

available, simplifying the design considerably. The Microchip MCP73837 was chosen (datasheet at ⊘/Hardware/Datasheets/Powersupply/MCP73837. pdf). The MCP73837 offers total management of a single cell lithium ion battery, with several user configurable settings. The DSP can determine the state of the battery manager and control it via GPIO pins. The battery manager is set with a resistor to limit charge current to 1 A (0.5 C) from a DC source. The USB charge current default is 100 mA(0.05 C), but can be set to 500 mA(0.25 C). A thermal shutdown is also implemented with an NTC resistor.

When dealing with batteries, knowing the remaining capacity is important to indicate low power. The capacity available in the cell is directly but not linearly proportional to its voltage. Because of this relation the resolution of any battery voltage measurement will affect how well the remaining capacity can be determined. The DSP has several internal ADC's and it is convenient to use one of these to measure the battery voltage. The DSP's ADC's can be combined internally to make a single 12-bit SAR(successive approximation register) convert resulting in a $\frac{3.3 \text{ V}}{2^{12} \text{ bits}} = 806\mu \frac{\text{V}}{\text{bit}}$ count. The voltage range on a lithium cell is V_B: 2.75-4.2 V. This range exceeds the ADC maximum voltage and must be lowered to ensure proper operation. Lowering the maximum battery voltage to the maximum ADC voltage is achieved via resistive voltage division. A ratio of $\frac{3.3 \text{ V}}{4.4 \text{ V}} = 0.786$ is required, this ratio is estimated using E96 value resistors: 78.7k $\Omega \cdot 0.786 = 61.9$k Ω. This signal conditioning results in a V_B range of 3.3-2.16 V on the ADC, which in turn yields $\frac{\Delta V_B}{\text{count}} = \frac{3.3 \text{ V} - 2.16 \text{ V}}{806\mu \frac{\text{V}}{\text{bit}}} = 1414.98$ counts.

Using a belt-and-braces approach, a backup is implemented in case 1415 counts is insufficient. The main disadvantage of using the resistive voltage division is limited range due to the voltage offset of the range. To resolve this a simple op-amp configuration is used after the resistive divider to subtract the offset and gain the signal to the full ADC range (see schematic E.8): $2.5 \cdot (0.786 \cdot V_B - 2.16 \text{ V})$ resulting in a 0.154-3.03 V range which yields a $\frac{3.03 \text{ V} - 0.154 \text{ V}}{806\mu \frac{\text{V}}{\text{bit}}} = 3569.73$ counts. Reading the battery voltage and battery manager state allows the DSP to make decisions regarding battery.

To allow the system to charge and run at the same time, a MOSFET switch and a schottky diode (PMFPB8032XP) is added as recommended by Microchip in application note *AN1149.pdf* (⊘/Hardware/Datasheets/ PowerSupply/). The two charge inputs are connected to the MOSFET and separated by two very low forward voltage (360 mV) schottky diodes (PMEG3010EP) in a configuration that disconnects the battery voltage when a greater charge voltage is present. Datasheets and application note is available at ⊘/Hardware/Datasheets/PowerSupply/.

3.10.3   Regulator

The system is battery operated, so a high efficiency regulator is preferable. Running the system directly off a battery is possible, if the battery is carefully selected. It is however inconvenient regarding the analog sections. As analog circuits operate as a ratio of the supply voltage, regulation is required to ensure predictable operation. This allows the system to be calibrated as needed by the transparency requirement. The calculation in 3.10.1 only gives a working estimate of the system requirements, and the power supply regulation must be designed with some margin to suppress transient noise on the shared power rail.

A low-dropout linear regulator is the most common regulator, it is inefficient but incredibly simple to implement. A low dropout regulator can never regulate higher than a few hundred millivolts below its input voltage. This is a problem because of the battery voltage drop when it is discharged. Linear regulators are better suited for using Ni-MH which have a very flat discharge voltage curve.

The recommended lithium ion battery regulation topology is switched mode power supply. A switched mode supply allows the battery to discharge to its drop out voltage (2.75 V) while maintaining a regulated 3.3 V rail. Switch mode supply efficiency is unmatched, easily performing more than 90%. This efficiency comes with increased noise. Switching regulators are in their nature noisy, so it is important to be able to filter the inevitable noise. This can be achieved by having a very high switching frequency, orders of magnitude higher than the systems analog band is preferable. The TPS63001 is chosen (⌾`/Hardware/Datasheets/PowerSupply/TPS63001.pdf`), it has a switching frequency of 1.25M-1.5M Hz which is far above the operating range of the analog circuits and can supply at least 3.3 V at 0.8 A from a 1.8-5.5 V voltage range. The efficiency of the converter is characterized in the data sheet in the following major worst case 3.3 V output efficiencies:

- 2.4 V_{in} >70% at 2 mA
  >90% at 100-400 mA
  >80% at 400-800 mA
  >75% at 800-1000 mA

- 4.2 V_{in}
  >75% at 2 mA
  >90% at 100-1000 mA

All values are estimated from TPS63001 figure 2 page 6 of the data sheet (⌾`/Datasheets/Powersupply/TPS63001.pdf`). From the values specified an expected efficiency of at least 80% is expected. The system power is controlled by disabling the regulator with a simple switch as indicated in figure 3.19. This does mean that the system will have a very small battery drain, even when powered off, of about 7 μA from the MCP73837, 1 μA from TPS63001 and possibly 1 μA from PMFPB8032XP resulting in a 9-7 μA standby drain. The drain is insignificant, and the battery has a safety

threshold preventing it from discharging below 2.75 V.

3.10.4   Layout Considerations

Low noise design is partly attributed to hardware layout. To this end the entire circuit is heavily decoupled. All analog sections reside on a separate power plane decoupled between two 2nd order low pass filters as can be seen in the schematic in E.8. The analog power plane is derived from the main power supply and has its own power connection traces directly routed from the regulator. This power plane supplies all analog circuitry and is also available on the input and output headers.

The CODEC is only available in a DFN package and because of this and the size constraints of the portable nature of the system, every device is specified in a DFN or similar package. This results in a very thin board and allows for larger battery within the case.

The final board for the processing platform can be viewed in figure 3.20 and the hear through device in figure 3.21.
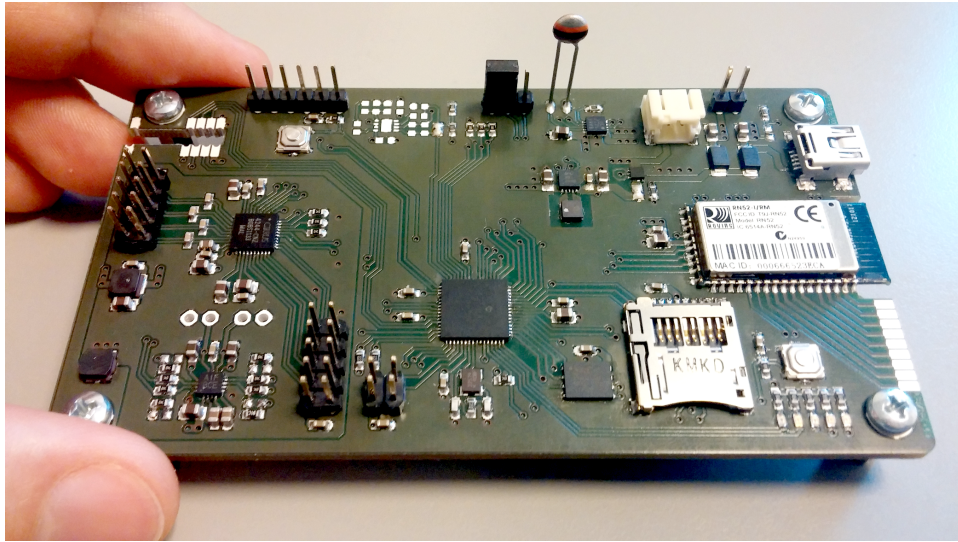
Figure 3.20: Final board implementation. User interface and case not shown.
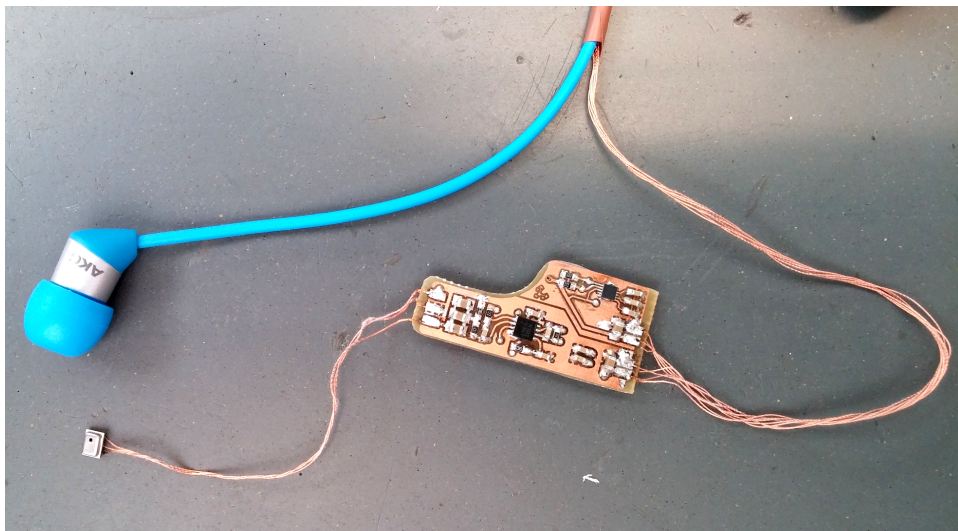

Figure 3.21: Final hear through device implementation.

Chapter 4

Implementation

This chapter gives a short description of the elements implemented on the system. First a description of the implemented equalizers and how they are quantized, and handled in the DSP. The next part describes the implemented head tracker and how the magnetic field is translated into a direction. The next section describes the incorporation of the virtual source and how it is filtered to include directional information. Finally an overview of the implemented program is shown and the flow of the program is elaborated. The implemented filter structure can be viewed in figure 3.2.

4.1   Filter Implementation On DSP

The FIR filters designed are represented by coefficients. The coefficients derived from MATLAB are signed 64 bits integers, these are not applicable to the DSP which operate in signed 16 bits (twos compliment). This implies the need for quantization so the filter coefficients will be represented by 1 sign bit and 15 fractional bits. However reducing the amount of bits to represent a coefficient also reduces the accuracy of the actual value of the filter coefficient. This will have an effect on the precision of the filter response in the system.

   The filter coefficients are quantized to signed 16 bit in MATLAB and then converted to hexadecimal using a built-in function in MATLAB, and saved to a file for the specific filter. The Bluetooth module on the processing platform is utilized to receive the coefficients as a raw binary file. The coefficients are then saved the internal serial flash memory. This ensures that the filters only have to be transferred once, and can be easily accessed or changed changed. The Bluetooth utilizes the build-in UART on the DSP which handles the data and sends it via the SPI bus to the serial flash memory. The filters could have been saved to the DSP's internal memory. But as the serial flash already contains the HRTF database the filters are also put here for coherency. The program used for uploading filters can be

seen at ⊙/`Software/Upload.X`.

On system start-up the filter coefficients for the two equalizing FIR filters are read from the serial flash memory and moved to the internal memory of the DSP. They are set up as two coefficient buffers in the coefficient memory area.

4.2   Head Tracking

The head tracking is implemented with the magnetometer. The magnetometer has a build-in configuration register to determined the amount of samples per second. The maximum sampling rate is 80 times a second. However if fewer readings are acceptable the magnetometer features the possibility to do oversampling. This ensures an averaged readout which is more stable than a fast readout. The register is implemented with a readout frequency of 20 Hz and an oversampling rate of 64 times per readout. A necessity of the magnetometer is to calibrate it. Of-the-shelf it has no actual reference point for the three axis (X,Y,Z) and the readouts are not valid. To secure that the magnetometer has a zero reference point, the minimum and maximum readings of each axis is found. This is done in order to find the dynamic range of each axis. An offset of the dynamic range is implemented to ensure that the magnetometer returns both positive and negative values of the magnetic field centered around zero. The offsets implemented for each axis of the magnetometer is:

- $X_{\text{offset}} = 855$
- $Y_{\text{offset}} = -218$
- $Z_{\text{offset}} = -196$

The values listed is the offset count of the magnetic field value for each direction. Each count represents a magnetic field of 0.1 μT, this value is calibrated from the factory and is used for calculating the value of the resulting vector in the magnetic field. It should be noted that the calibration counts only applie to this specific magnetometer.

The magnetometer returns three values each represents the value of the magnetic field in their respective direction. The implemented system uses only a two dimensional vector space as the direction of interest is only in the horizontal plane. The placement of the magnetometer inferes that the values needed for computation of direction is the Y and Z values. The raw values of the magnetometer give no direction but merely a value of the magnetic field. To be able to index the HRTF filters correctly a direction in degrees is necessary, this is done with the following trigonometric relation:

$$\frac{180}{\pi} \cdot arctan\left(\frac{Y}{Z}\right) \tag{4.1}$$

The value returned by *arctan* is in radians, and is converted to degrees. This equation will return a value between -180 and 180 which in total covers the entire horizontal plane. It should be mentioned that depending on the orientation of the hear through device the input to the *arctan* should be revised to compensate for the third axis offset.

4.3 Virtual Source

The virtual source is implemented as a single input buffer. The signal is filtered through the appropiate HRTF to obtain the directional cues that are normally a result of the pinna. This results in an output that can be merged with the sound already processed from the microphone and equalizer.

The source for the virtual source buffer can be accessed from different inputs. The CODEC has two unused channels that can be used as an input as long as the input is supplied differential. The implemented system supports the Bluetooth interface. This makes inputting the virtual source easy. The sound recieved by the Bluetooth module is recieved by the DSP. The digital stream is stored in the signal input buffer before filtering.

4.4 HRTF Filtering

The ability to place the virtual source in the horizontal plane is achieved by filtering the virtual source signal with the appropriate HRTF. The HRTF's implemented are obtained from the VALDEMAR database created at AAU [Christensen., 2000]. The database consists of over 12000 measurements with an impulse response length of 256 samples. The measurements covers the entire sphere whith the horizontal view divided into an interval of 2 degree. The measurements are sampled with a frequency of 48 kHz and stored as MATLAB .mat files.

For implementation on the processing platform some preprocessing in MATLAB is necessary. The system designed features a sampling frequency of 44.1 kHz which is not aligned with the 48 kHz of the VALDEMAR database. In order to use the database HRTF's the responses are re-sampled to 44.1 kHz in MATLAB. This is important because implementing the 48 kHz sampled version would eg. introduce a longer ITD as the measured impulse responses contain these. Filtering at 44.1 kHz would increase the delay as there are more samples than needed and furthermore alter the frequency response wanted. The re-sampled responses are converted to binary files so

it is possible to transfer the filter coefficients via the Bluetooth serial interface. The code for re-sampling and creation of binary files can be found at ⊙/Matlab/HRTF_sweep/coef_resamp.m. The filters are not included on the CD as they are the property of AAU (Access can be granted by the acoustics department).

The filters used in the implementation has a FIR length of 200 words, which is more than needed for representing the aural cues [Blauert, 2005]. The filters are implemented with their respective delay included in the filter start, this ensure a correct ITD for each direction. The amount of filters needed to represent a full 360 degree horizontal plane is 360 filters as there are two filters from each direction one for each ear. To minimize the size of the filterbank the implemented filters only include the horizontal left plane. It is still possible to get a full 360 degree experience as the implemented filters are the same for the right side as long as the ears are mirrored, and as long as symmetry is assumed for the human head. This results in a filterbank containing 90 sets of HRTF's to cover the horizontal plane with an resolution of 2 degrees.

The filtering of the virtual signal is done by fetching the wanted filter in the filterbank on the serial flash memory and then convolving the virtual signal for each ear before the signal is merged with the signal from the microphone.

4.5 Program

The program is designed in two parts. The main loop handles the input from the magnetometer and fetches the correct filters. The second part is interrupt driven and handles the filtering of the relevant inputs.

In figure 4.1 the main routine is depicted in a flowchart. Before the main program is started the initialization of the different modules are setup. This include setup of the system including the ports and busses needed for communication. After the system set up the perphial modules including codec, magnetometer, headphone amplifier and Bluetoth module is setup. Included in the setup is fetching the microphone and headphone filter coefficients as these filter are constant through the program. The last point in the initialization enables the DCI interrupt.

After initialization the main loop starts. The first step is a check of the magnetometer status, if the magnetometer has a new sample (indicated by a status bit in the device) the routine starts calculating the heading of the listeners head. After the heading is determined the correct filter adress on the flash is calculated and the filter is fetched into the internal memory of the DSP. The filter coeffcients are loaded in to the respective coefficient buffers which are utilized by the interrupt routine. Depending on the heading the coefficients are loaded in reverse order so the filter channels are switched in

order to accompany the mirrorring of the HRTF database as mentioned. A
double buffer scheme is implemented to prevent the interrupt from using a
filter that is not ready. The filter will be put in buffer A or B depending
wich one was used last. The active filter is controlled by the main loop, and
the interrupt checks this via a software flag. After the filter coefficients are
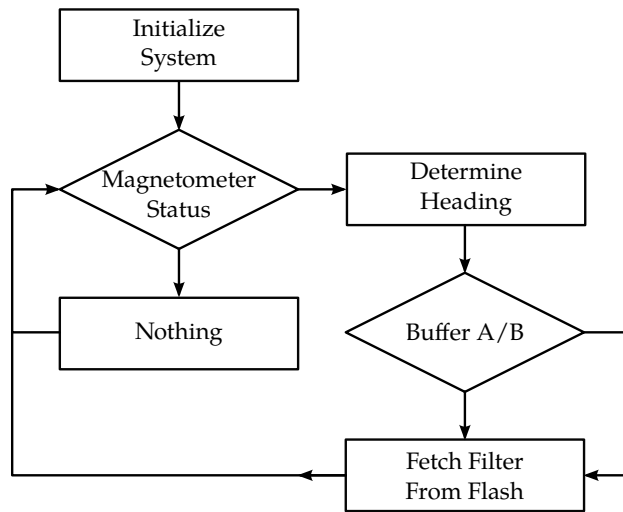fetched and loaded the routine returns to the magnetometer and waits for a
new readout.

Figure 4.1: Main program loop flowchart

The interrupt routine is programmed in assembly to accomodate the
speed required for realtime applications, furthermore the DSP features spe-
cific assembly routines for filtering. The assembly program is a sequential
program and the filtering of the different inputs could have been done in
reverse order with no effect. The interrupt flow can be viewed in figure 4.2.
After an interrupt occures the virtual signal is fetched at the SPIbuffer and
arranged in a signal buffer containing only the virtual signal. After the signal
buffer the signal is convolved with the coefficients contained in the the filter
buffer. This is done both for the right and left coefficient buffer to synthesize
the binaural signal from the virtual mono signal recieved. The two signals
are stored awaiting merging with the processed microphone signal.

The samples from the microphones are collected from the DCI buffer
and arranged in two signal buffers. The filter coefficients for the microphone
equalizer are convolved with each of the signal buffers returning two filtered
versions of the microphone signals. These signals are then merged with the
binaural virtual source signal. The merged signal is then convolved with
the headphone equalizer filter coefficients, and then moved to the transmit
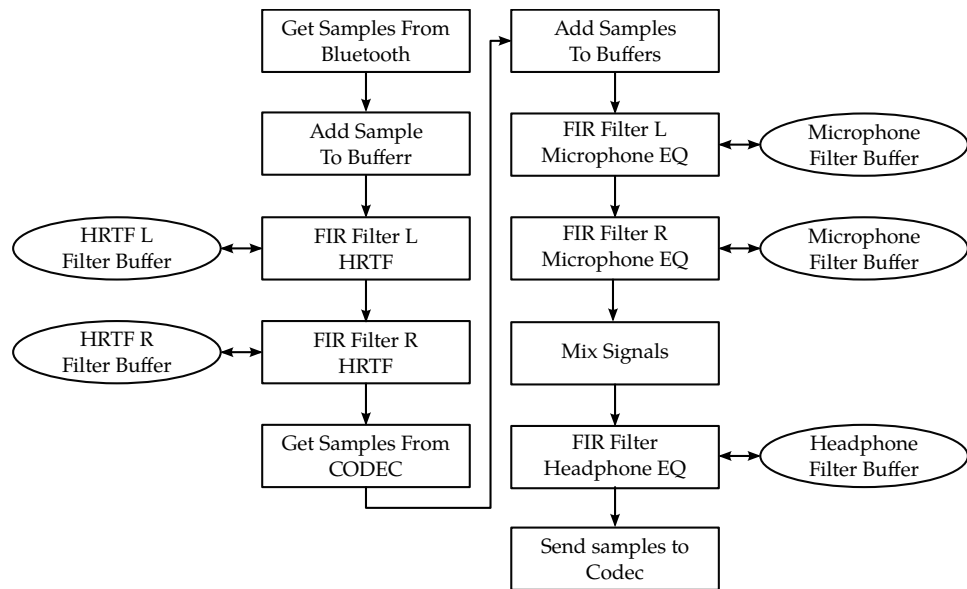buffers of the DCI module which sends the processed signal to the CODEC.

Figure 4.2: Interrupt program flowchart

Chapter 5

System Verification

This chapter verifies the implemented hardware design and software design. The verification will include measurements of calibrate system transparency. The readouts of the magnetometer will be assessed. During the verification of complete system no power saving modes are utilized on the DSP.

5.1 Transparency

To verify transparency the system is first calibrated. The measured filter characteristics are compared to the designed filters in 3.1.2 and 3.1.3.

System Calibration

The system sound level is verified at a calibrated known input. The system is verified at 94 dB 1 kHz for transparency, this value is chosen as the filters are normalized to 1 kHz and therefore will not influence the calibration.

The following table shows a complete list of the equipment utilized to perform the measurement.

Type	AAU-number	Brand	Model
Complete system	-	CB/RE	Version 1
Microphone amplifier	08022	B&K	Type 2636
Microphone pre-amp	06558	B&K	Type 2627
Measurement microphone	06552	B&K	Type 4144
Coupler Artificial ear	07902	B&K	Type 4152
Frequency analyzer	08596	B&K	Type 2133
Microphone calibrator	08373	B&K	Type 4230

The coupler is calibrated with the B&K calibrator to ensure a 94 dB level with no system mounted. The system is then setup with the headphone mounted to the coupler and the microphone to the calibrator. A readout

on the frequency analyzer yield the following result before calibration of the entire system.

- Uncalibrated Left: 106.6 dB
- Uncalibrated Right: 106.6 dB

The uncalibrated values are approximately 12 dB above the input signal. The calibration to 94 dB is done digitally in the DSP dividing the processed signal. The same measurement is done with the new calibration parameter and yield the calibrated result:

- Calibrated(-12dB) Left: 94.4 dB
- Calibrated(-12dB) Right: 94.4 dB

The calibrated result are close to the input value of 94 dB. The small variations can be due to the nature of the coupler which is not fitted for in-ear headphones. The reached value is within reasonable limit of the 94 dB mark and is accepted as a calibrated measure of the system output. But most importantly the levels are equal.

System Response And THD

The system amplitude response and the total harmonic distortion (THD) is verified. The test is done with both the calibrated and uncalibrated system but with no filters used. This reflects the total amplification in the system from microphone entrance to headphone amplifier output. In order to obtain the responses the NI-PCI audio analyzer (AAUnr: 64640) is used. In figure 5.1 the amplitude response of the entire system is shown. The electrical gain of the system in the passband is 34 dB. This is in accordance with the value calculated in 3.7.
The calibration of the system should decrease the total electrical gain 12 dB. In figure 5.2 the system amplitude response is shown after calibration. As expected the total electrical gain is 22 dB, 12 dB lower than uncalibrated.
The THD of the calibrated system is shown in figure 5.3. It is higher than expected, but still acceptable and inaudible. The amount of THD could be attributed to the measurement system poor ability at low voltage levels to some degree.

Filter Characteristics

In order to verify the filter characteristics designed in 3.1.2 the systems frequency response is analyzed with only the microphone placement filter enabled. Figure 5.4 shows the frequency response of the system. It is observed that the response corresponds to the designed filter, it should be noted that the overall higher amplitude is due to the amplification of the system straight
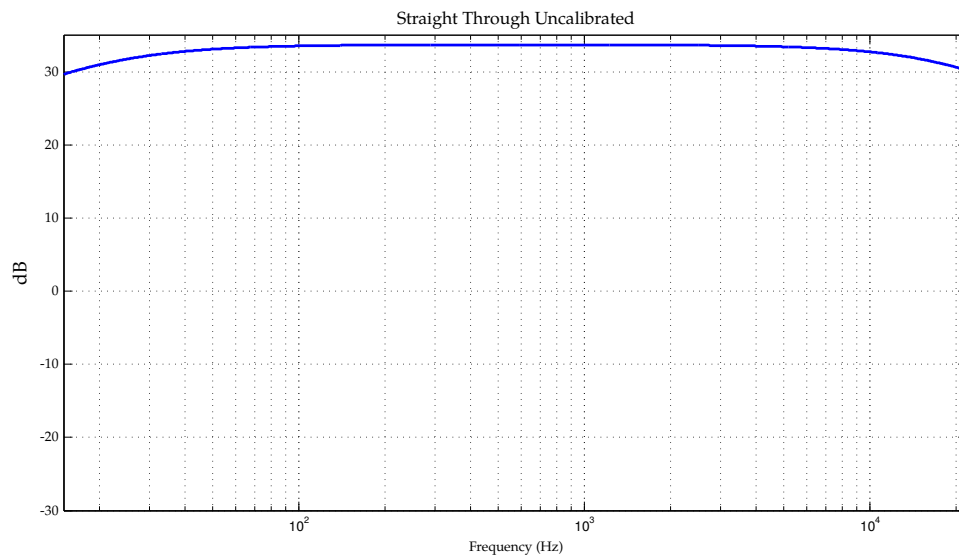
Figure 5.1: Uncalibrated system response without any equalizing filters from 15 Hz to 22 kHz.
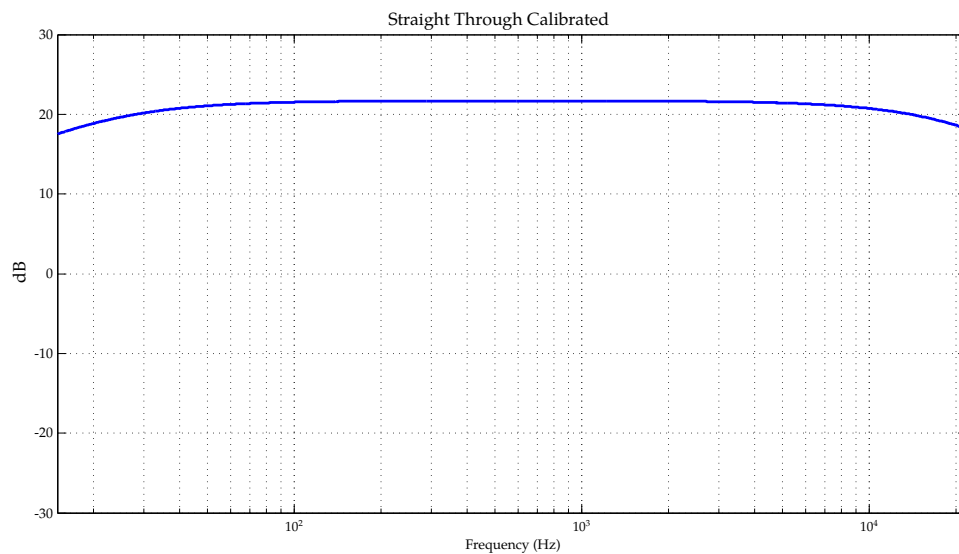

Figure 5.2: Calibrated system response without any equalizing filters from 15 Hz to 22 kHz.

through as shown above. Due to broken equipment (Headphone coupler), the filters are only charetarized electrically.

The same test is performed only changing the filter from the microphone equalizer filter to the headphone equalizer filter. The frequency response measured can be seen in figure 5.5 and fits well with the designed filter in 3.1.3.
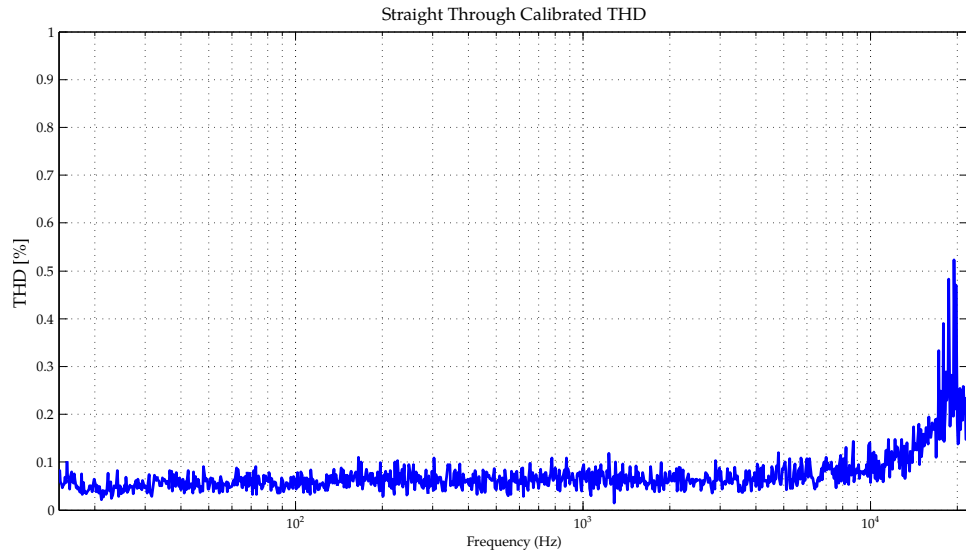
Figure 5.3: System THD without any equalizing filters from 15 Hz to 22 kHz.
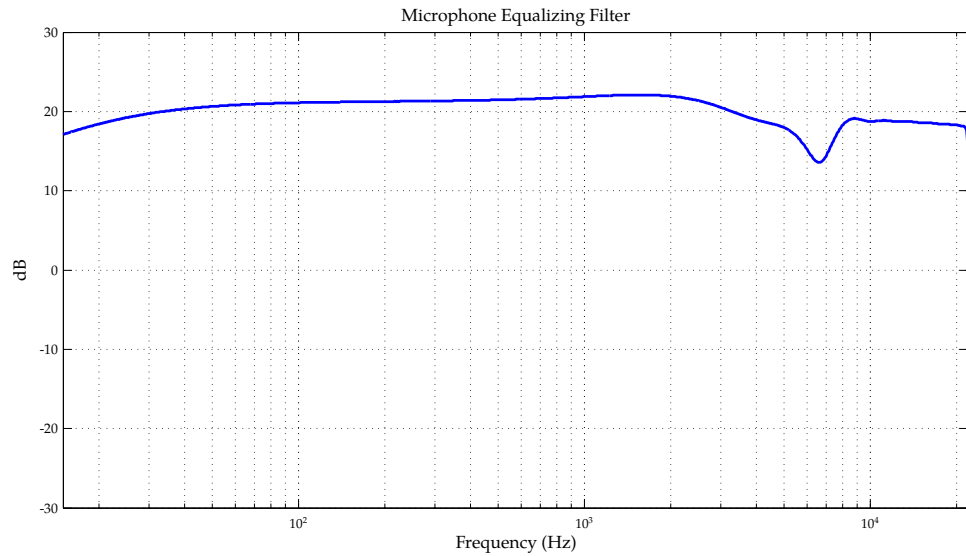
Figure 5.4: System response with microphone equalizing implemented.

All graphs in the previous is shown with the same axis as the ones used in the design sections. There is however one exception for figure 5.1 which has a different axis in order to show the uncalibrated response. The results can be plotted using the following program in MATLAB located at ⊙/Hardware/ Tests/Plot_testresults.m. The raw measurements are also located in this folder. The program used for the processing platform is located at ⊙/Software/Main_test/. The code includes all filters uncommented. For the specific tests, the filters can be uncommented.
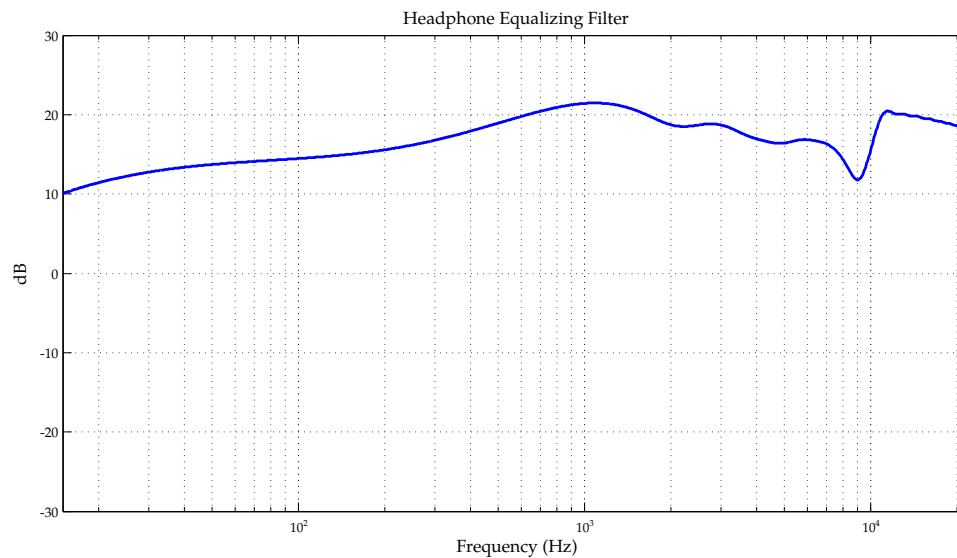
Figure 5.5: System response with headphone equalizing implemented.

5.2 Magnetometer

The function of the magnetometer is tested via the Bluetooth connection to a terminal window on a computer. The test is setup by holding the magnetometer in upright position and then turning it. The readout from the terminal window shows that the range is between -180 degrees and 180 degrees. It is of utmost important to keep the magnetometer in upright position because any tilt of the magnetometer will inflict the readout. The test is done after calibration of the magnetometer and shows good performance compared with a compass. The magnetometer is rotated 45 degrees and the readout is compared to the compass. The test is performed several times to ensure reliability of the measurement. The program for the test is located at ⊙/Software/Magnetometer.X.

Chapter 6

Conclusion And Discussion

6.1 Project Summary

Throughout the project a hear through device and a processing platform was developed. The system is developed based on the theory discussed in chapter 2. The main parts of the spatial hearing is discussed and several aspects of human sound localization is investigated. The main points were binaural cues, monaural cues and dynamic cues.

Several measurements were done in the prestudy to understand and document the changes occurring in the directional cues when normal hearing is replaced by a hear through device.

The main part of the project was the design and development of the hear through device and the processing platform. Several parameters such as transparency and wearabillity have been the main design features throughout the system design. A large part of the development is based on the measurements and the equalizing filters needed for the system transparency.

Verification of the subsystems was performed and all of them were satisfactory. Unfortunately the system could not be verified as intended because of unfortunate equipment failure.

6.2 Conclusion

The main project points defined in the project description are evaluated in the following:

- **Calibrated system**
  The system must accurately reproduce any sound pressure within the normal hearing range.
  The implemented system has a natural sound reproduction, the sound level through the system is within 0.4 dB. The availible microphones did not allow for the entire dynamic range to be covered however.

- **Transparrent**
  The system must allow the users normal hearing.
  Several measurements confirm the electrical accuaracy of the reproduced signal. But due to the mentioned equipment faliure the filtering could not be verified as intended. The system does have a very natural sound when wearing it. Subjectively the system feels very transparent.

- **Source**
  The system must seamlessly infuse a stationary virtual source.
  The system can infuse any source recieved form the Bluetooth connection and mix it into the signal path. The HRTF filtering is implemented and works as expected resulting in an authentic directional sensation caused by the binaural synthesis. The magnetometer works and gives accurate headings as long as the third axis offset is not to large. Time constraints however did not allow verification of the virtual source stationarity.

Every subsystem of the entire system is availible and tested individually. However more time would have allowed for further measurements and test of the final combined subsystems. Time constraints forced the implementation to be simplified to only handle the horizontal plane.

6.3   Discussion

The developed system platform is build with the abillity for further reaserch in mind. This is the reason for including through documentation on the developed hardware and the user manual included (appendix E).

During the project several solutions for the hear through device have been discussed but not documented. Due to time and money constraints ideas such as impedance controlled artificial eadrums and specialized caste head-phones were not considered for implementation. The processing platform however is a good oppertunity to investigate these excotic devices further.

Further software development on the system platform would include in-corporation of reverberation. As discussed in chapter 2 adding reverbaration to the sound would prevent the virtual signal from collapsing inside the head. Reverbaration would require further investigation of the algrithms and their paramaters. Recall from the introduction that paramater extractsion is men-tioned. A major complication in implementing reverbaration is matching the reverbaration already present in the real signal.

The system design was prototyped and tested thoroughly. Several pro-totypes were built before the final PCB's were ordered. All of the hardware subsystems have been individually tested to avoid errors on the final board. The final version of the system was tested with the implemented software to ensure the functionality of the developed software and hardware.

We are very pleased with the result of the project and hope that others can benefit from it.

Chapter 7

Bibliography

AKG. Akg k323xs. `http://dk.akg.com/akg-product-detail_dk/k323xs-blue.html`, 2014. Accessed: 2014-05-11.

Durand R. Begault. *3-D Sound For Virtual Reality and Multimedia*. Academic press Inc., 1994.

J. Blauert. *Spatial Hearing*. MIT Press, 1999.

J. Blauert. *Communication Acoustics*. Springer, 2005.

Bjarke P. Bovbjerg Pauli Minnaar Xiaoping Chen Jan Plogsties Claus Vestergaard Flemming Christensen. Measurement report, 2000. Requires acces to the VALDEMAR 2DEG database at AAU.

Flemming Christensen, Pablo F. Hoffmann, and Dorte Hammershøi. Measuring directional characteristics of in-ear recording devices. In *Audio Engineering Society Convention 134*, May 2013. URL `http://www.aes.org/e-lib/browse.cfm?elib=16784`.

Aki Härmä, Julia Jakka, Miikka Tikander, Matti Karjalainen, Tapio Lokki, Heli Nironen, and Sampo Vesa. Techniques and applications of wearable augmented reality audio. In *Audio Engineering Society Convention 114*, March 2003.

H. Klensch. Beitrag zur frage der lokalisation des schalles im raum. *Pflügers Arch*, 250:492–500, 1948.

Tomasz R. Letowski and Szymon T. Letowski. *Auditory Spatial Perception: Auditory Localization*. Army Research Laboratory, 2012.

Catarina Mendonça, Guilherme Campos, Paulo Dias, José Vieira, João P. Ferreira, and Jorge A. Santos. On the improvement of localization accuracy with non-individualized hrtf-based sounds. *J. Audio Eng. Soc*, 60(10):

821–830, 2012. URL `http://www.aes.org/e-lib/browse.cfm?elib=16555`.

Henrik Møller, Michael Friis Sørensen, Dorte Hammershøi, and Clemen Boje Jensen. Head-related transfer functions of human subjects. *J. Audio Eng. Soc*, 43(5):300–321, 1995. URL `http://www.aes.org/e-lib/browse.cfm?elib=7949`.

Carsten Niemitz, Maike Nibbrig, and Vanessa Zacher. Human ears grow throughout the entire lifetime according to complicated and sexually dimorphic patterns — conclusions from a cross-sectional analysis. *Anthropologischer Anzeiger*, 65(4):pp. 391–413, 2007. URL `http://www.jstor.org/stable/29542890`.

Lauri Savioja, Jyri Huopaniemi, Tapio TAPIO Lokki, and Riita Väänänen. Creating interactive virtual acoustic environments. *J. Audio Eng. Soc*, 47 (9):675–705, 1999.

Willard R. Thurlow and Charles E. Jack. Certain determinants of the ventriloquism effect. *Perceptual and Motor Skills.*, 36(3c):1171–1184, 1973.

F. E. Toole. In-head localization of acoustic images. *J. Acoust. Soc. Am.*, 48(4):943–949, 1970. URL `http://dx.doi.org/10.1121/1.1912233`.

Appendix A

Microphone Placement

Purpose

The purpose of the following measurements is to determine the optimal placement of the microphone on the shell of the headphone by comparing with a blocked entrance reference measurement.

Method

To asses the impact of microphone placement in the ear with the headphone protruding from the ear canal a reference is needed for comparison. The reference measurement is done as a blocked entrance measurement without the headphone. Then the headphone is inserted into the ear canal and the microphone is attached to it at a specified angle and a multi directional(25) MLS measurement is performed. When all measurements have been performed an average difference from each microphone position is calculated relative to the blocked entrance reference. All measurements are done with the same microphone as only the relative difference is of interest, and differing microphone characteristics would complicate the data analysis.

Twenty five microphone positions will be characterized. Each position will be characterized from twenty five identical sources distributed on a hemisphere at 700 mm from the artificial ear as illustrated in figure A.3 and A.4. The microphone is placed at angles relative to the entrance of the ear canal of approximately 0°, 45°, 90°, 135° and 180° azimuth and altitude respectively, to ensure coverage of the entire hemisphere of the headphone case. Figure A.1 and A.2 illustrate the microphone positions that will be investigated. A picture of the actual measurement setup in the anechoic chamber is shown in A.5. The placement of the microphone for the blocked entrance measurement with the artificial ear can be seen in A.6.
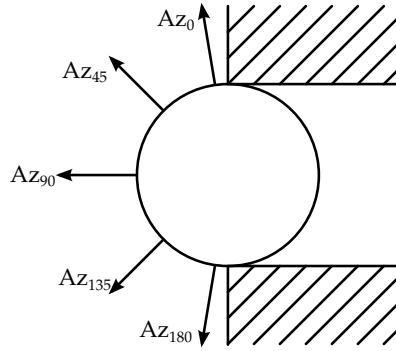
Figure A.1: Headphone blocking entrance to ear canal with microphone azimuth illustrated by normals $\theta_{\mathrm{Az}n}$. Left ear as seen form above.
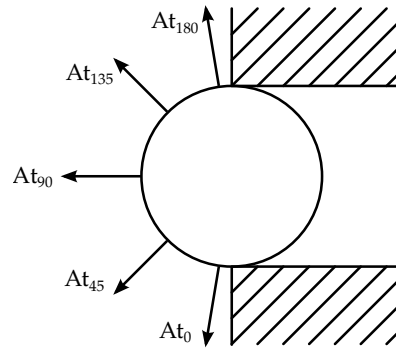

Figure A.2: Headphone blocking entrance to ear canal with microphone altitude illustrated by normals $\theta_{\mathrm{At}n}$. Left ear as seen form the front.
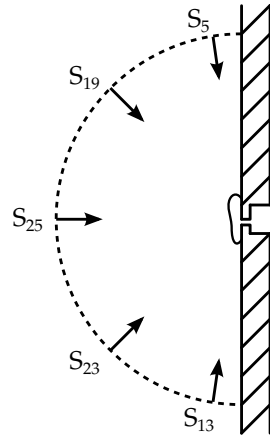

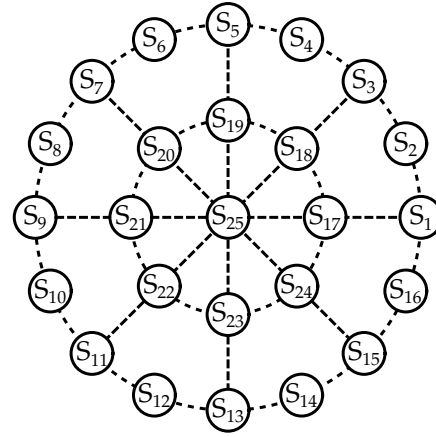**Figure A.3:** Artificial ear mounted in infinite baffel with source altitude illustrated. Left ear as seen form the front.

Figure A.4: Speaker distribution on the spider hemisphere.

Equipment

The following is a complete list of the equipment utilized to perform the measurements.

Figure A.5: The spider setup in an anechoic chamber.

Figure A.6: Artificial ear with the microphone mounted for blocked entrance reference measurement.

Type	AAU-number	Brand	Model
Microphone	-	Wolfson	WM7120
Microphone power	-	AAU	Special unit
Microphone amplifier	33654	B&K	Nexus
Amplifier	08340	Pioneer	A-616
Soundcard	56533	Edirol	UA-5
Acquisition unit	76944	Hewlett Packard	Akulab 18
Microphone calibrator	08373	B&K	4230
Ear	-	AAU	Anja
In-ear Headphone	-	AKG	K323XS
Spider	-	AAU	25 speakers

Corrections

The method specifies 25 different positions to be measured. During the measurement setup some difficulties were encountered. This section will explain the corrections made to the method, and some additional measurement-points.

Initially the setup aimed for a total coverage of the hemisphere. The positions chosen for test are not all achievable. This is due to the geometry of the space that the in-ear headphone occupies. The pinna will interfere with

the microphone port. The measurements that are achievable are done. Furthermore a study of microphone placements in the concha are tested as well as one position on the outside of the ear. Photos of all microphone positions tested can be seen viewed at 🌐`/Appendicies/Appendix_A/Images/`.

Results

This section will cover the results of the measurements. All the results are compared to the initial reference measurement for the 25 speaker positions with the microphone mounted at a blocked entrance. In figure A.7 the complete reference measurement is shown. Each color correspond to one of the 25 different speaker positions. As can be seen in figure A.7 the measurements have a clear high pass tendency. This is caused by the speakers used in the spider, the speakers have a poor response at low frequencies which is documented in [Christensen et al., 2013].
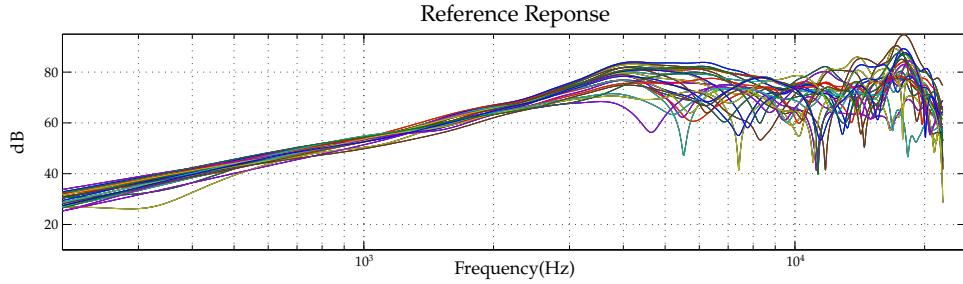
Figure A.7: Reference transfer functions, measured at blocked entrance for all 25 speaker positions.

The difference between the reference measurements and each microphone position measurement is assessed in the following. For each microphone position the average difference is found between each speaker and the corresponding reference measurement. An average is then determined by the resulting 25 averages. This average result can be seen in table A.1.

The results from the average method does not give an accurate view of the difference in characteristics. Another assessment method is chosen in order to visualize the deviation between the reference measurement and the different microphone position measurements. In figure A.8, A.9 and A.10 the deviation between the reference and the microphone positions are seen. All microphone positions are located on the ear bud itself and Az(azimuth) and At(altitude) are relative to straight ahead and the horizontal plane.

In figure A.11 The deviation between the reference measurement and microphone positions in and on the ear is seen.

|dB|	Az_0	Az_{45}	Az_{90}	Az_{135}	Az_{180}
At_0	-	-	-	-	-
At_{45}	-	-	-	-	4.08
At_{90}	2.19	3.32	3.45	4.25	2.71
At_{135}	-	-	7.03	7.77	7.43
At_{180}	-	-	-	-	7.03

Table A.1: Microphone response average difference from blocked entrance reference. Beside the averages in the table 3 measurements on the ear is performed. The result for these measurements are: Outer ear 5.69, bottom inner ear 5.59 and top inner ear 4.80.

The microphone positions deviations are very different compared to each other. In figure A.12 the positions with the most homogeneous deviations are seen and these will be the base for further investigation of the microphone position in order to define one position for the final system. The MATLAB program used for data analysis is found at ◉/Matlab/Mic_place_analasis/Mic_placement.m
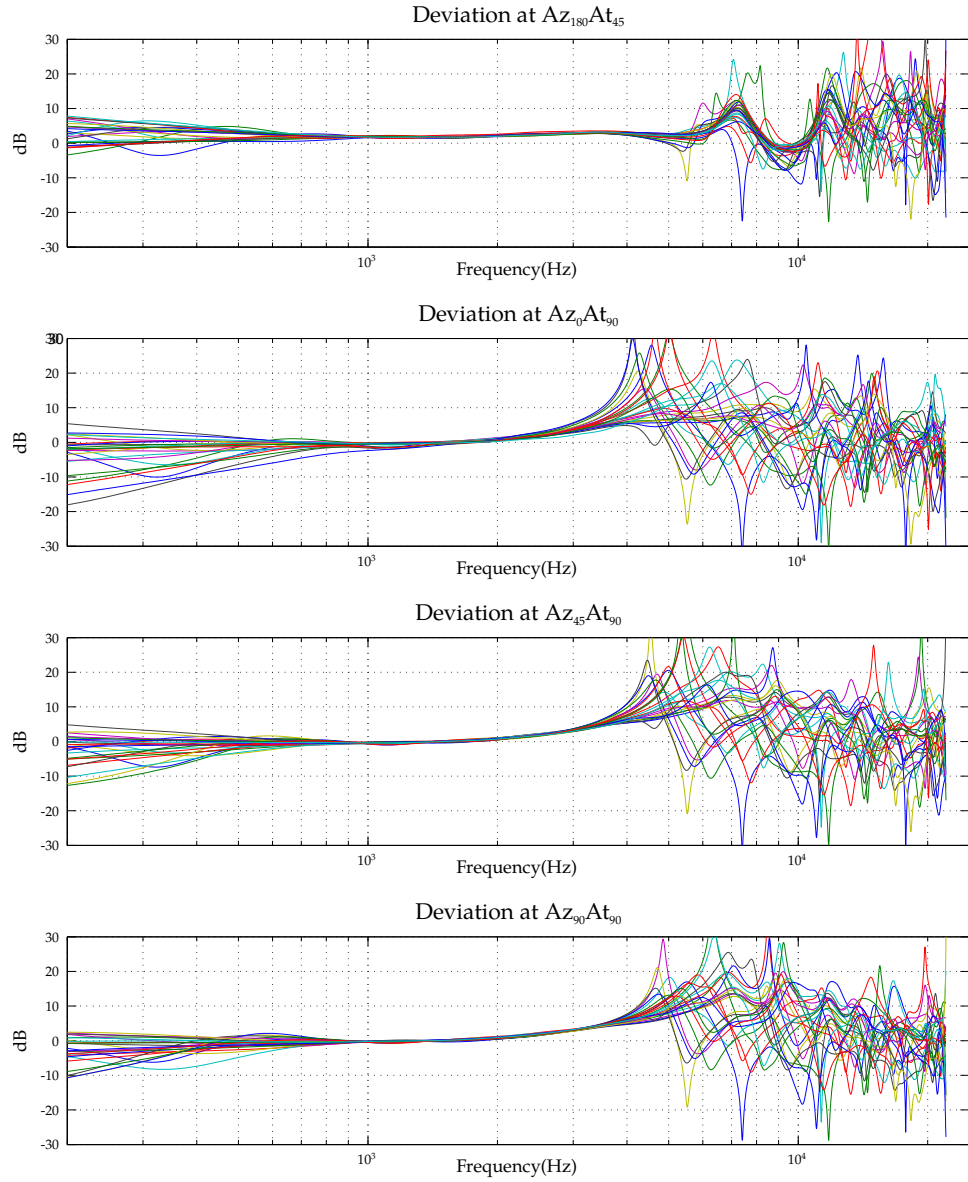
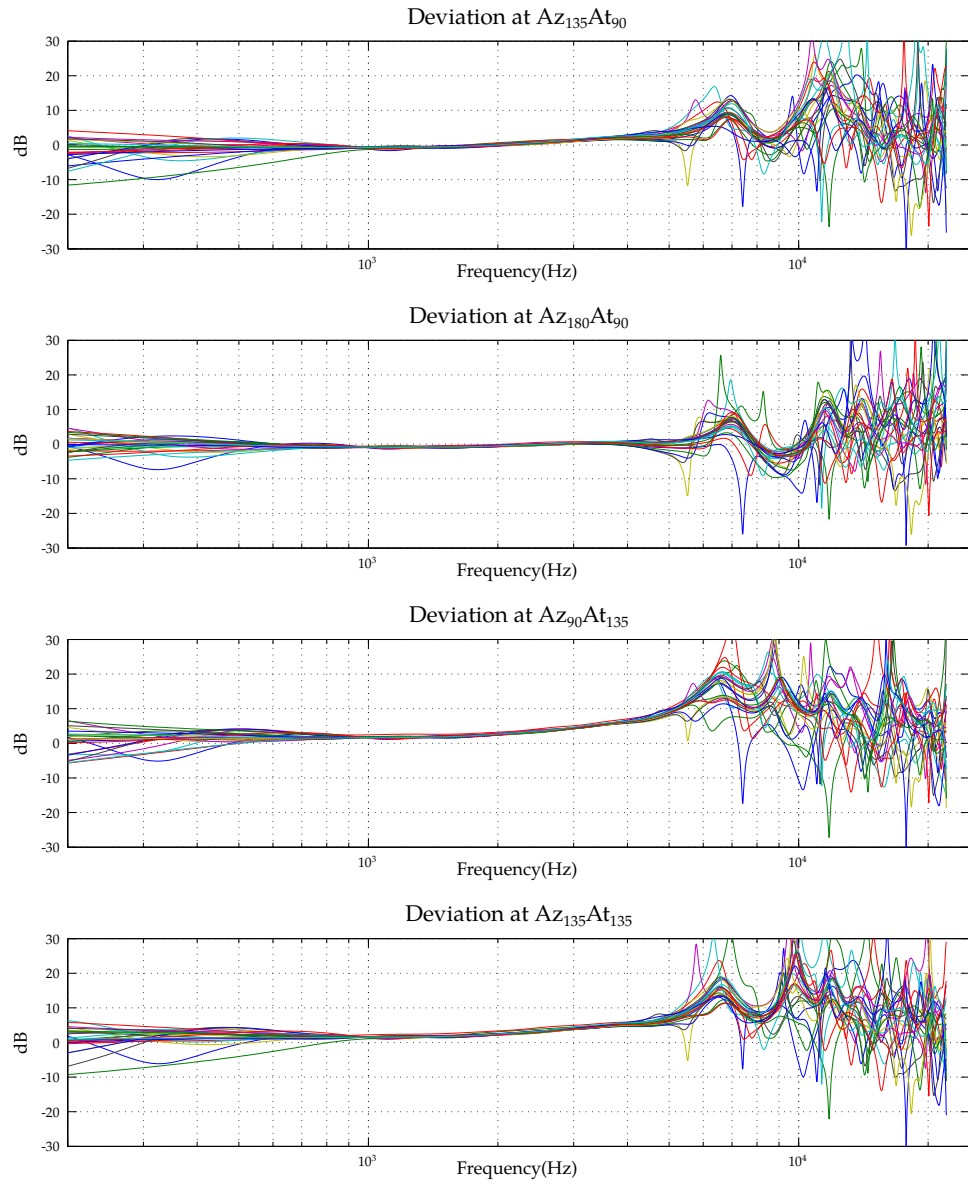**Figure A.8:** Deviation between the reference and microphone positions on the earbud.

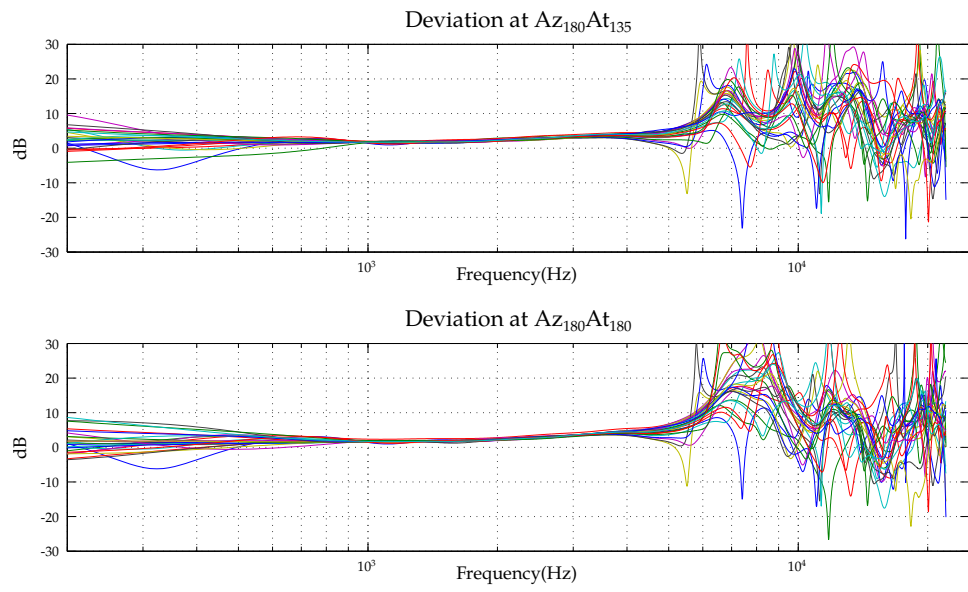**Figure A.9:** Deviation between the reference and microphone positions on the earbud.

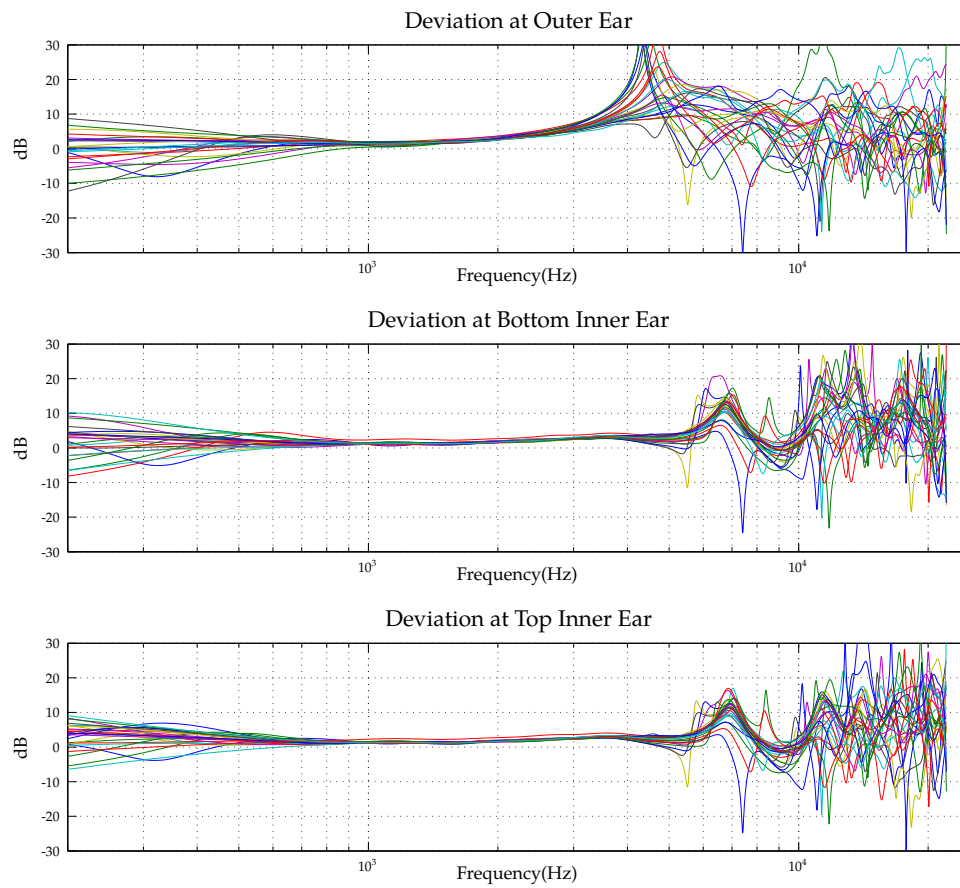**Figure A.10:** Deviation between the reference and microphone positions on the earbud.

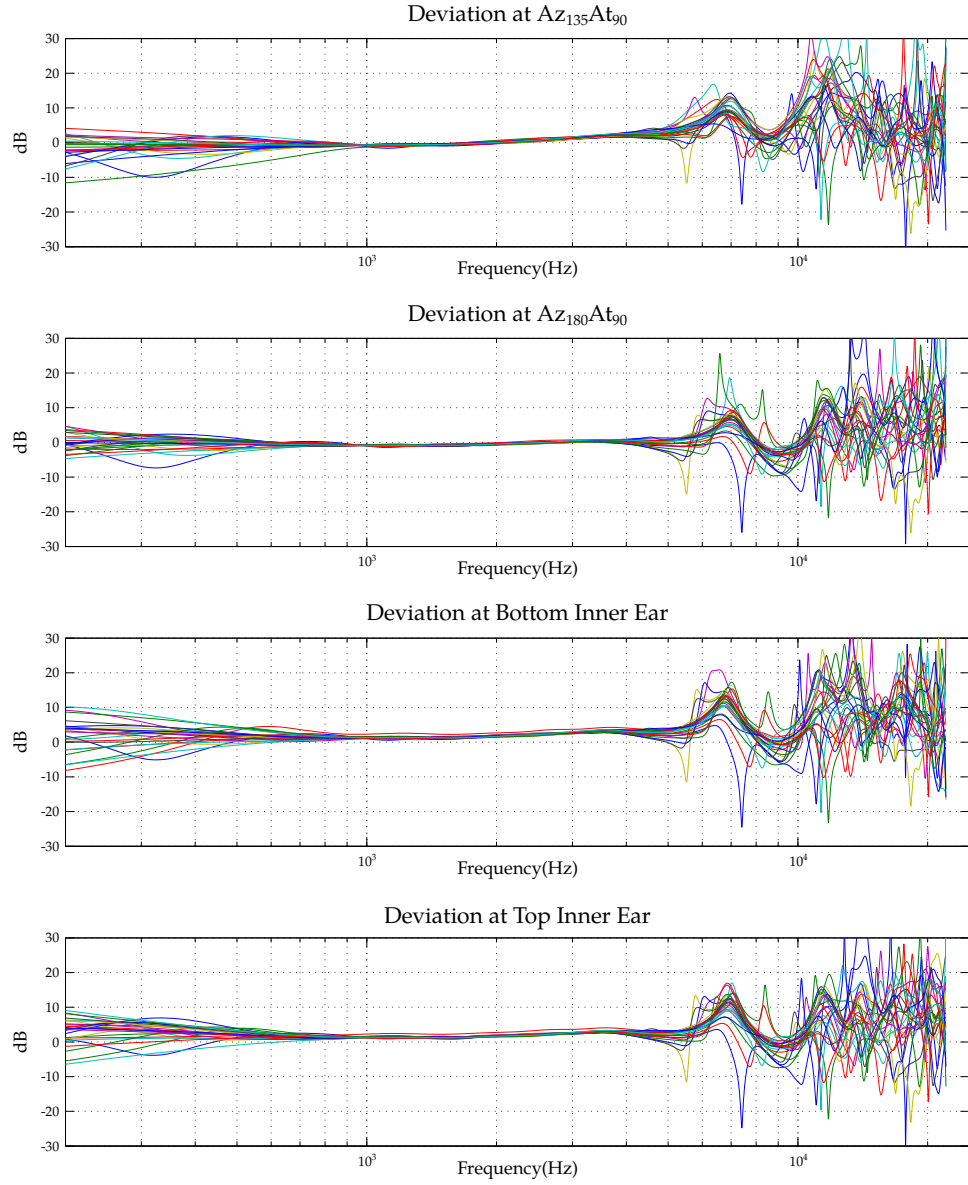**Figure A.11:** Deviation between the reference and microphone positions in and on the ear.

Figure A.12: Deviation between the reference and microphone positions the 4 best positions.

Appendix B

Short Study Of Human Pinnae Variance

Purpose

The purpose of the following measurements is to determine the acoustic variance of human pinnae.

Method

The pinnae will be charaterized following the method used in appendix A eg. a multidirectional MLS measurement. Only the blocked entrance measurement is performed. Five to ten subjects of different gender, ages 20-60, will be used as a representative population. The large spread in age is attributed to the continious growth of human ears [Niemitz et al., 2007]. As the chareteristics of the pinna is directional, it is critical that each measurement is done with the same placement of each pinna, to minimize errors. To simplify the comparison only the orthogonal directions will be investigated. This was chosen as the directional cues are assumed to be most pronounced from these directions. The extremum features of the following locations and the variance of theese features is to be determined: S_1 (front), S_9 (back), S_5 (top), S_{13} (bottom), S_1(side) (see figure A.4).

Equipment

The following is a complete list of the equipment utilized to perform the measurments.

Type	AAU-number	Brand	Model
Microphone	-	Wolfson	WM7120
Microphone power	-	AAU	Special unit
Microphone amplifier	33654	B&K	Nexus
Amplifier	08340	Pioneer	A-616
Soundcard	56533	Edirol	UA-5
Acquisition unit	76944	Hewlett Packard	Akulab 18
Microphone calibrator	08373	B&K	4230
Ear	-	AAU	Dorthe
In-ear Headphone	-	AKG	K323XS
Spider	-	AAU	25 speakers

Results

The results of the measurement are based on the participating subjects. The subject gender and age is noted for reference, all the subjects can be seen in table B.1. Subject one is the artificial ear and is used as the reference measurement, this measurement secures a fixed ear reference. All other subjects are mounted to the baffel but sligth movements can occur during the measurement. Subject sevens measurement are discarded as they obviously have some error. All the measurment are avalible at ⊚/Appendicies/Appendix_B/. For each subject a picture of the microphone placement and the pinna can also be found at ⊚/Appendicies/Appendix_B/Images/. The response of each subject is compared to the reference. In the reference each notch in the frequency response is determined as these are directy related to the geometry of the pinna. Each subjects response is then compared and the frequency of corresponding notches are noted. This is then used as a measure of the variation of the pinnae.

Subject	Gender	Age
1	F	
2	M	28
3	F	24
4	M	29
5	M	26
6	F	56
7	F	22

Table B.1

The result of subject one is shown in table B.2. The values are extrapolated from the graphs shown in B.1, B.2, B.3, B.4 and B.5. The values are found at each notch and will serve as a guideline for the other subjects notches. The pinnae variations of the subjects are shown in B.3 as a minimum and

Reference	1. notch kHz	2. notch kHz	3. notch kHz	4. notch kHz
Front	7.5	10.2	15.6	-
Top	15.5	-	-	-
Back	7.9	14.5	-	-
Bottom	5.6	9.7	12.6	16.4
Side	8.5	14.2	-	-

Table B.2

maximum value found for the subjects. The MATLAB program used in the analysis can be found at ⊙/Matlab/Pinna_variations/Pinna_variation.m

Variation	1. notch kHz	2. notch kHz	3. notch 3 kHz	4. notch kHz
Front	6.2 - 7.1	8.6 - 10.4	11.4 - 17.7	-
Top	10.3 - 15.9	-	-	-
Back	7.9 - 9.2	12.5 - 15.1	-	-
Bottom	5.2 - 6.0	9.2 - 9.9	12.0 - 13.9	15.2 - 18.9
Side	7.6 - 9.3	12.0 - 15.4	-	-

Table B.3
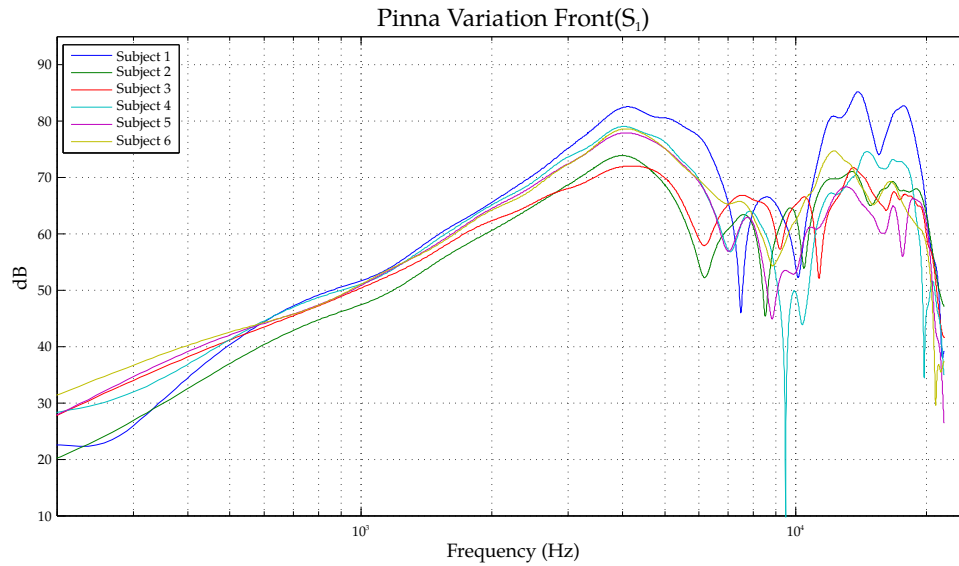
Figure B.1: HRTF of the 5 subjects including subject 1(reference), front direction(S_1).
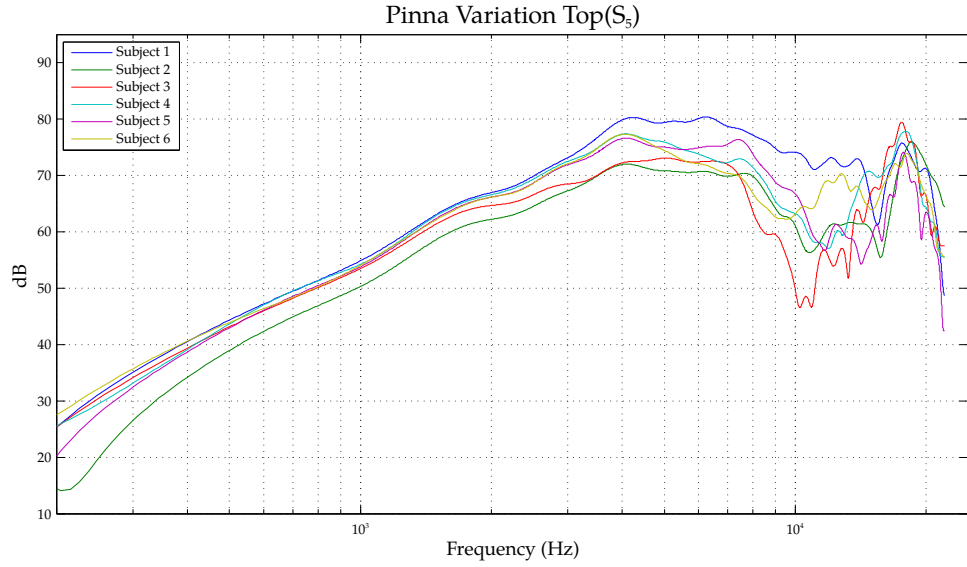
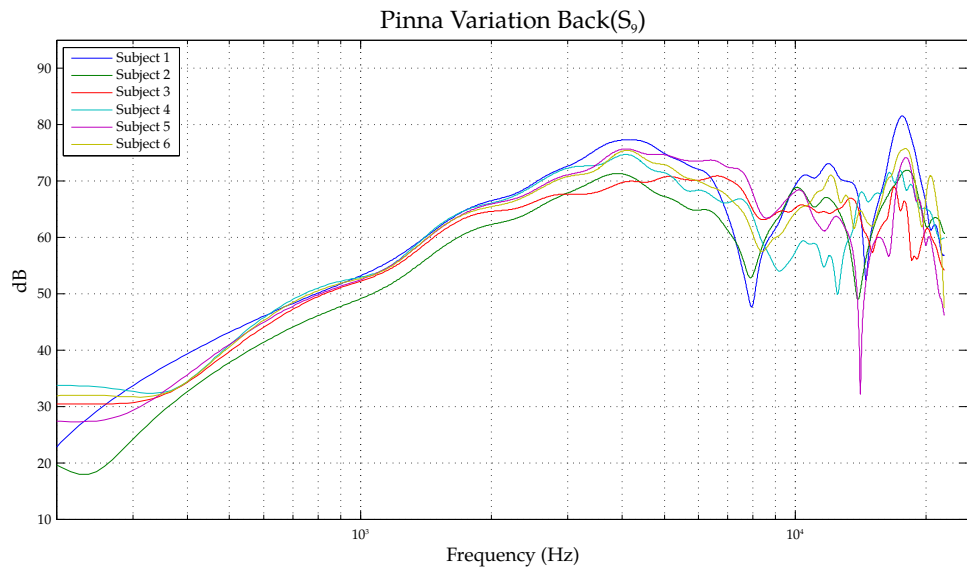**Figure B.2:** HRTF of the 5 subjects including subject 1(reference), top direction(S_5).

Figure B.3: HRTF of the 5 subjects including subject 1(reference), back direction(S_9).
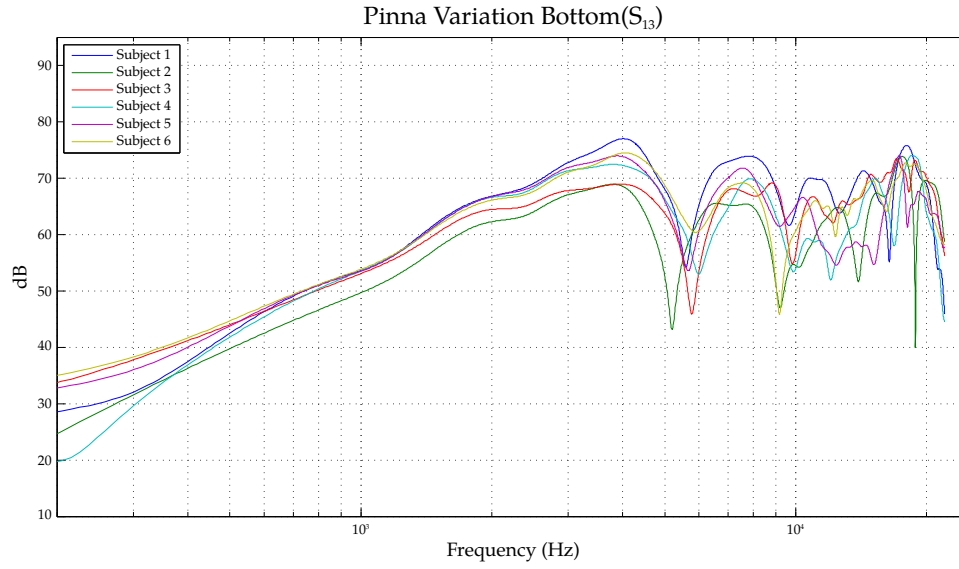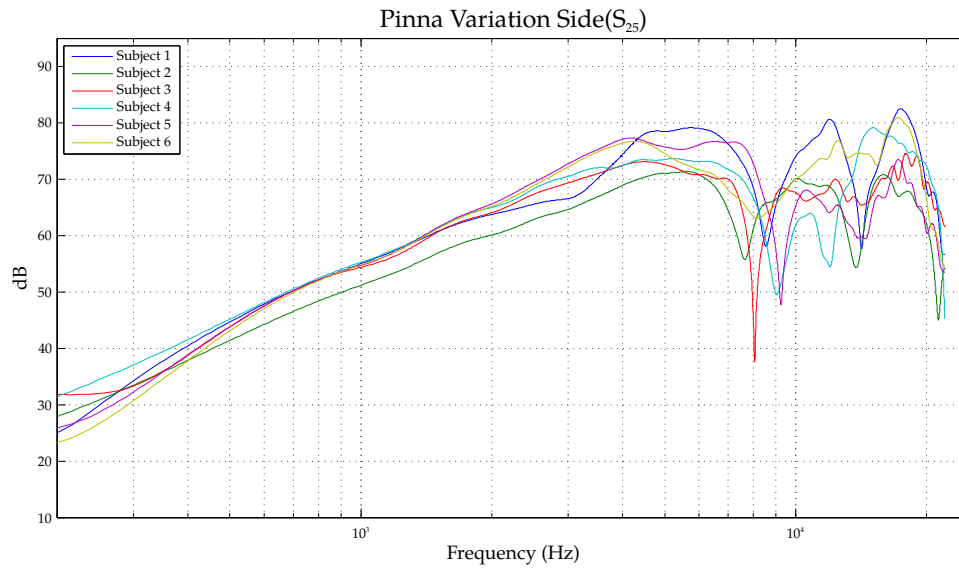
Pinna Variation Bottom(S_{13})

Figure B.4: HRTF of the 5 subjects including subject 1(reference), bottom direction(S_{13}).

Pinna Variation Side(S_{25})

Figure B.5: HRTF of the 5 subjects including subject 1(reference), side direction(S_{25}).

Appendix C

Headphone Damping

Purpose

The purpose of the following measurement is to determine the insertion loss caused by wearing headphones.

Method

The insertion loss caused by wearing headphones will be determined using a standardized audiometry measurement performed on two subjects. The subjects are tested without headphones first to determine the actual hearing threshold. The headphone is then mounted and a second audiometry is performed. The magnitude response of the reference and the second audiometry are compared. The differences in the magnitude is an expression of the damping of the headphone.

Equipment

The following is a complete list of the equipment utilized to perform the measurements.

Type	AAU-number	Brand	Model
Audiometer	07630	Madsen	OB 40
In-ear Headphone	-	AKG	K323XS

Table C.1: Full list of equipment used for the measurements.

Results

The audiometry measurements are illustrated in figure **??**. The subjects were normal hearing males, 26 and 28 years of age. The measurements show a clear low pass tendency below 3 kHz. An average hearing loss of 23.2 dB can be found from the measurements. The measurement data and relevant software can be viewed on ◉/Appendicies/Appendix_C/.
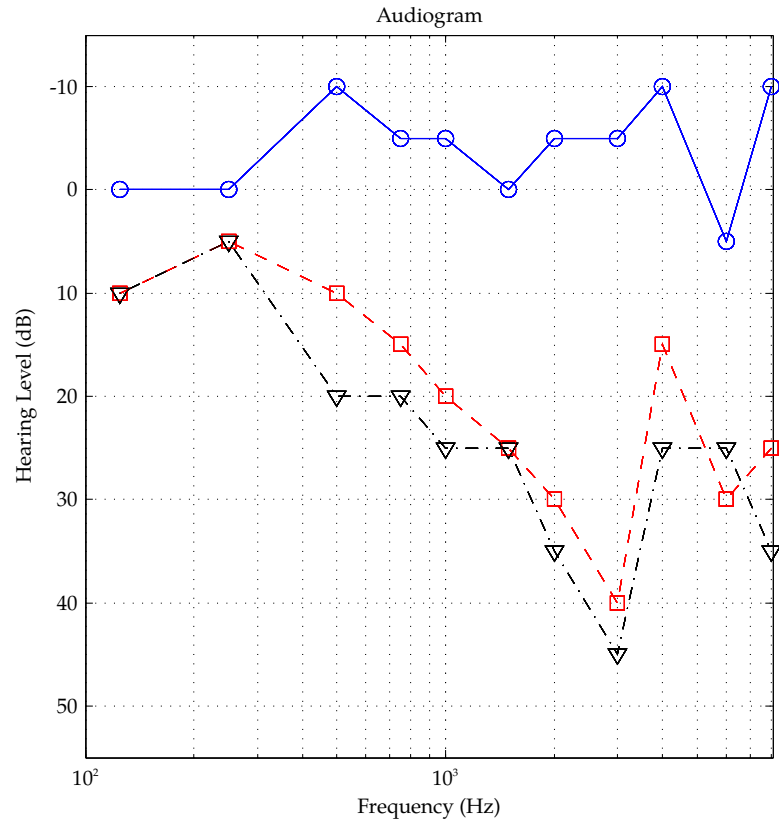

Figure C.1: Subject 1 audiometries with and without ear canal blocked by headphone. Blue circles mark the reference measurement. Red squares are blocked ear canal. Black triangles show the loss(Red and blue difference).
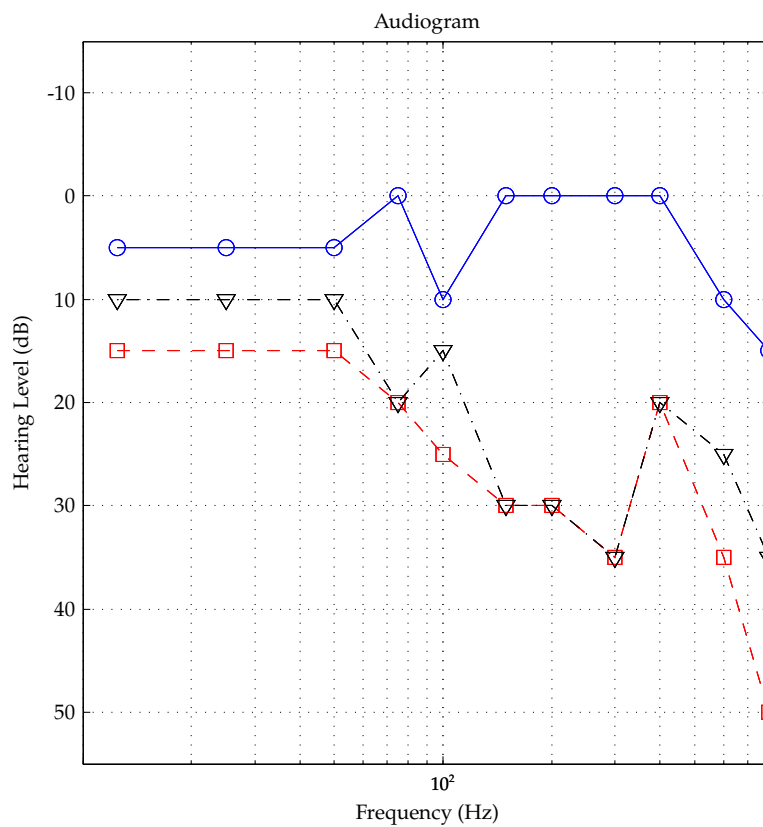
Figure C.2: Subject 2 audiometries with and without ear canal blocked by headphone. Blue circles mark the reference measurement. Red squares are blocked ear canal. Black triangles show the loss(Red and blue difference).

Appendix D

Headphone Measurements

Purpose

The purpose of the following measurements is to determine frequency response of the AKG K323XS headphone.

Method

The headphone is placed in a coupler connected to an MLS measurement system. The system is then used to determine the impulse response of the headphone. The MLS system is configured to measure at 44100 Hz (MLS order is 16). The impulse response is processed by an FFT in MATLAB to retrive the frequency response of the headphone.

Equipment

The following is a complete list of the equipment utilized to perform the measurements.

Type	AAU-number	Brand	Model
Measurement amp.	08717	B&K	2636
Coupler	65823	G.R.A.S.	26AC
MLSSA System	37493	-	PC Akulab33
In-ear Headphone	-	AKG	K323XS

Table D.1: Full list of equipment used for the measurements.

Results

Figure D.1 shows the frequency response of the AKG K323XS headphone. The response is derived from the impulseresponse generated by the MLS system. The measurement data and relevant software can be viewed at at ⊙/Appendicies/Appendix_D/
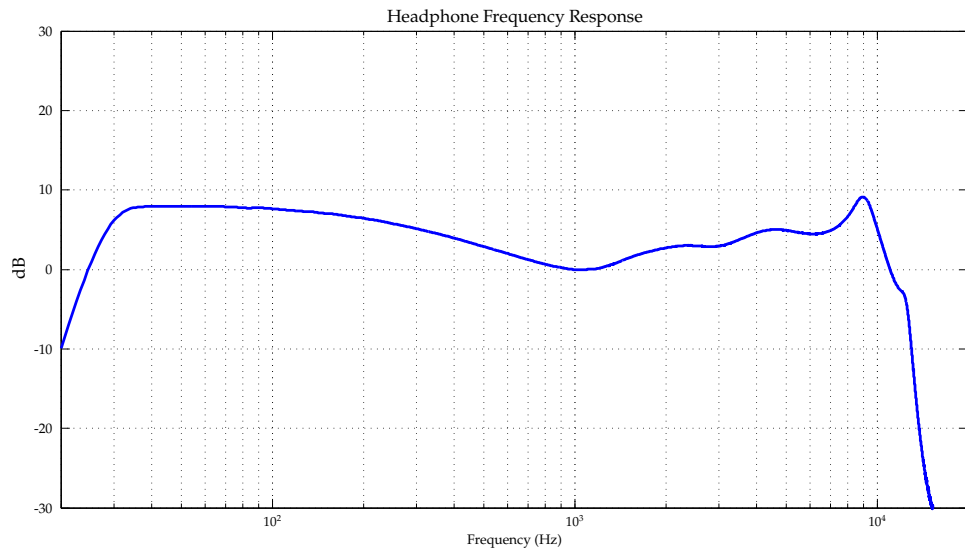

Figure D.1: Frequency response of the AKG K323XS headphonen normalized at 1k Hz.

Appendix E

System User Manual

This appendix serves as a reference for anyone wishing to use the hardware and software for further research and development. All hardware documentation is avalible at ⊘/Hardware/. This appendix contains an overview of the hardware and software and should allow the reader to get started developing applications. A software example is also made avalible.

E.1 Overview

Figure E.1 shows a simplified version of the processing platform. The main componentes are depicted together with all interface connections.

E.2 Hardware

Schematics and Board layout is done in Cadsoft Eagle(version 6.5.0). Eagle is a free(limited) schematics and board layout editor. Eagle is avalible at:

    http://www.cadsoftusa.com/download-eagle/

All hardware design document files are avalible at ⊘/Hardware/Eagle/ EEP10/. Aside from the board and schematic files a Library containing all parts of the project board is also made avalible at ⊘/Hardware/Eagle/ EEP10.lbr.

E.3 System Specification

All measurements are performed with full system running (no powersaving) from a 5 V supply with 125 mV$_{pp}$ noise with large transients.
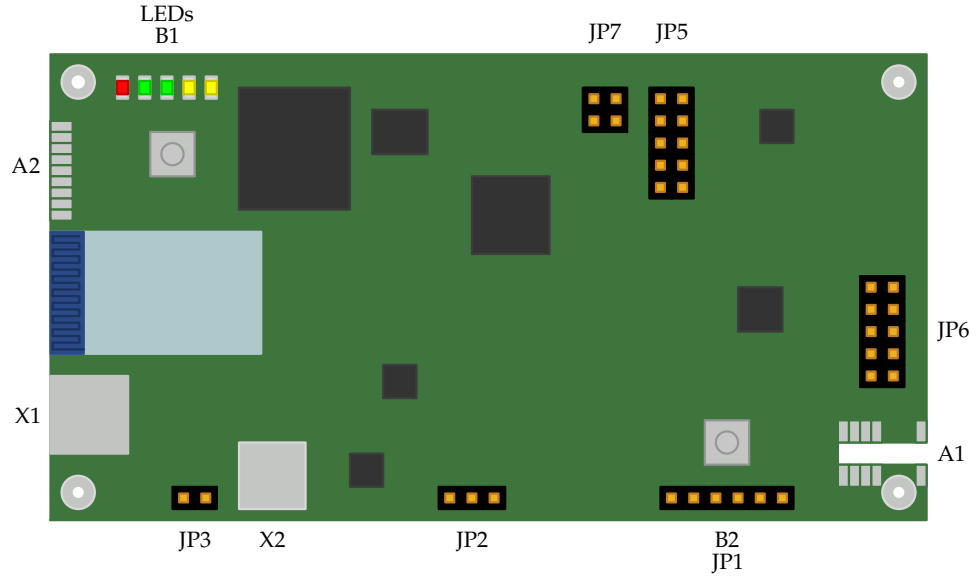
Figure E.1: Overview of the connections on the processing platform: **LED**'s: From left to right (Red and Green) Bluetooh status, (Green) Power, (2xYellow) system LED's, **B1**: system button, **JP7**: I2C, and digital power, **JP5**: CODEC differential output, **JP6**: Analouge supply and differential inputs, **A1**: I2C, button interface (JTAG), **JP1**: Programming and debug interface, **B2**: Reset Button, **JP2**: Switcher on/off, **X2**: Battery connection, **JP3**: External power supply, **X1**: USB, **A2**: Bluetooth analogue output (if enabled).

Measurement	Expected	Result	Notes
Battery Charge AC	1 A	1.133 A	
Battery Charge AC	1 A	1.043 A	System standby
System Voltage (Buck)	3.3 V	3.29 V	
System Voltage (Boost)	3.3 V	3.29 V	2.3 V_{in}
Regulator dropout	1.9 V	2.2 V	
System Voltage Noise	>50 mV_{pp}	31.3 mV_{pp}	5s average
Analog Supply Noise	>50 mV_{pp}	26.3 mV_{pp}	5s average
Total System Current	600 mA	132 mA	No power saving
System Clock	22.5792 MHz	22.578552 MHz	
Sample Rate	44.100 kHz	44.099 kHz	Calculated
DSP Instruction Clock	135.4752 MHz	135.471312 MHz	Calculated
System THD	<0.1%	<0.47%	20-20k Hz
Total Audio Path Offset	0 dB	± 0.5 dB	1 kHz, 94 dB

E.4 Software

The programmers reference manual *16-bit MCU and DSC Programmers Reference Manual.pdf* at ⚪/Software/ offers an overview of the internal structure of the DSP. It furthermore descibes the abilities of the DSP. The manual holds the instruction set for the assembly programming language, including a thourough describtion each instruction.

MPLAB X

MPLAB X is the programming and debugging platform for all Microchips devices. It supports in-circuit debugging with source code breakpoints, advanced stack trace and memory views, simulation, tight integration with the PICkit 3 amongst many other features. The current version(v2.10) is used in this project. The IDE is based on NetBeans and available for Windows, Linux and Mac, and can be downloaded free of charge at the following link:

```
http://www.microchip.com/pagehandler/en-us/family/mplabx/
```

The program is very intuitive and the built in help is very comprehensive. The users guide *MPLAB_ X_ IDE_ Users_ Guide.pdf* is a good place to start and can be found at ⚪/Software/.

XC16

XC16 is the free 16 bit device compiler supplied by Microchip. It is optimized for all 16 bit PIC's and is offered free of charge. The compiler can be used in an unlimited trail for 60 days, the unlimited version offers better optimization. The current version(v1.21) is used in this project. The XC16 compiler can be downloaded at the following link:

```
http://www.microchip.com/pagehandler/en-us/family/mplabx/
```

The complete documentation for the compiler *MPLAB XC16 C Compiler Users Guide.pdf* is located at ⚪/Software/. The user's guide gives an overview of the compiler specifics on how to define interrupts, mix assembly and c etc.

E.5   Zero To Blinky

Supplied on the project cd is a simple project example to get started. The code alternates the two user LED's state. It can be used as a template for any development on the platform and every pin is configured for the project board (the periphials are unconfigured). The software is supplied as an MPLAB X project at ⊙`/Software/Blinky` and should be opened with MPLAB X. Connect power and the debuger to the board before running the program by pressing the debug button at the top of the IDE.

E.6   Bluetooth

The Bluetooth module can be enabled by driving RD5 high. Once started the module will boot, and after a few seconds start alternating the Bluetooth status LED's to indicate that the module is discoverable. The module can be discovered by any Bluetooth device and will be listed as RN52-XXXX where XXXX is the last four digits of the MAC address printet on the module. The default configuration outputs any audio recieved to the analog pins at connector A2 as illustrated in figure E.1. This configuration can be changed by the DSP by asserting the /CMD(RF1) pin and sending the ASCII encoded command "S|,01" and a carridge return (the sequence [0x53, 0x7C, 0x2C, 0x30, 0x31, 0x0D]). Further information on the module and configuration is in *rn-bt-audio-ug-2.0r.pdf* avalible at ⊙`/Hardware/Bluetooth/RN-52/`.

The modules serial port is transparrent, connecting to the module will connect to the DSP's serial port. The port is configured at 115200 baud, 8 bits, No parity, 1 stop bit by default.

E.7 System Board Errata

The following section covers problems discoverd in the final board design. The user should read it carefully before assembling and powering the board.
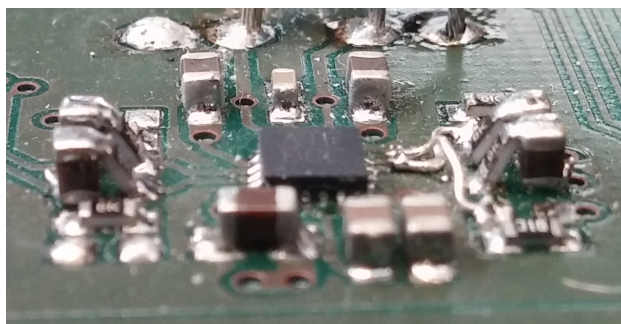
- **Issue Summary**
  - **Headphone Amplifier Connection**(U12): Pin 7 and 8 switched in footprint resulting in INR- and INR+ reversed.
  - **Work around**: Cut traces and rewire board as illustrated below:
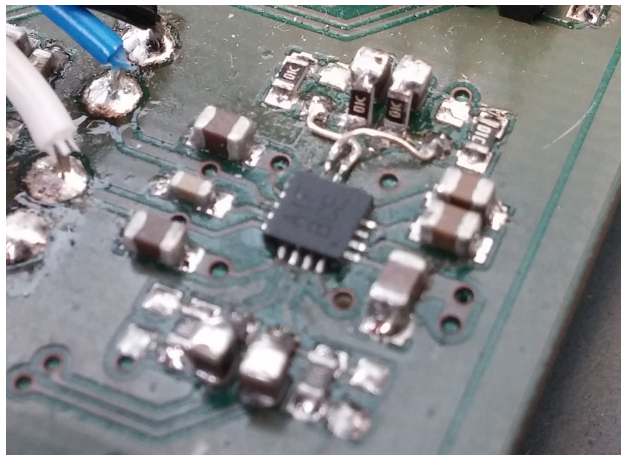
- **Issue Summary**
  - **Headphone Amplifier Input**: CODEC(U4) and headphone amplifier(U12) DC coupled.
  - **Work around**: AC couple CODEC and headphone amplifer with 1 uF as illustrated below:
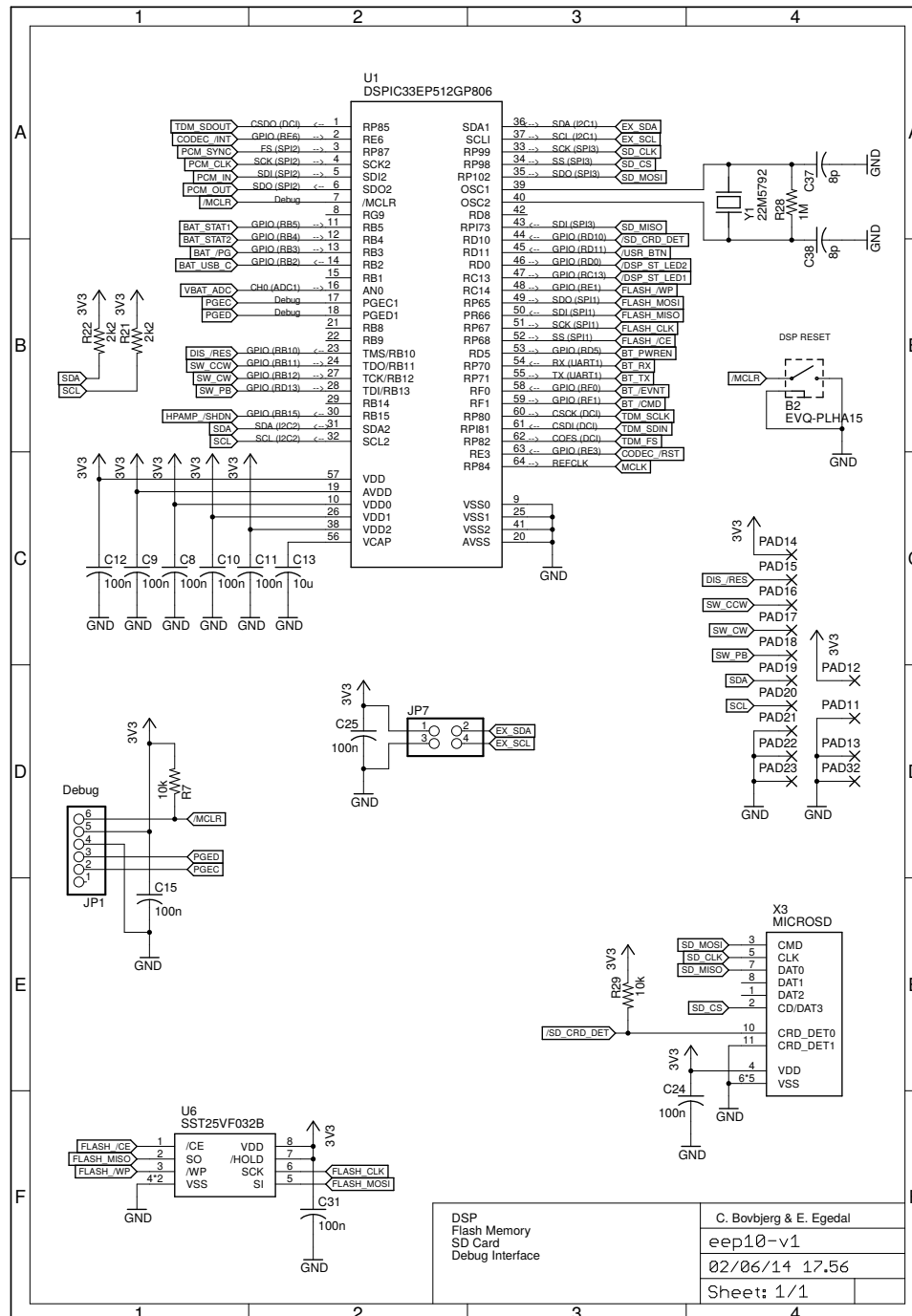
- **Issue Summary**

  - **Supply Voltage On Codec Header**: Missing Analog Supply on CODEC output header JP5 pin 9.
  - **Work around**: None, use Analog Supply from CODEC input header JP6 pin 9.

- **Issue Summary**

  - **Battery Voltage Amplifier**(U9): Datasheet not specific on wether or not the DFN pad is internally connected. Tested and working with pad connected to V_{DD}, but board footprint connected to GND. No internal connection can be measured on device. But remains untested on final board.
  - **Work around**: Do not populate battery voltage conditioner circuits. Use resistive voltage division only or change op-amp.

E.8 Schematic

DSP
Flash Memory
SD Card
Debug Interface

C. Bovbjerg & E. Egedal

eep10-v1

02/06/14 17.56

Sheet: 1/1

CODEC
Headphone Amplifier

C. Bovbjerg & E. Egedal

eep10-v1

02/06/14 17.56

Sheet: 1/1

Power Regulation
Battery Manager
Battery Voltage Sensing

C. Bovbjerg & E. Egedal

eep10-v1

02/06/14 17.56

Sheet: 1/1

Bluetooth Module
Status Leds
User Button
USB connection

C. Bovbjerg & E. Egedal

eep10-v1

02/06/14 17.56

Sheet: 1/1

User interface

C. Bovbjerg & R. Egedal

eep10-int-v1

02/06/14 18.03

Sheet: 1/1

Component Placement

Main Board Top Copper
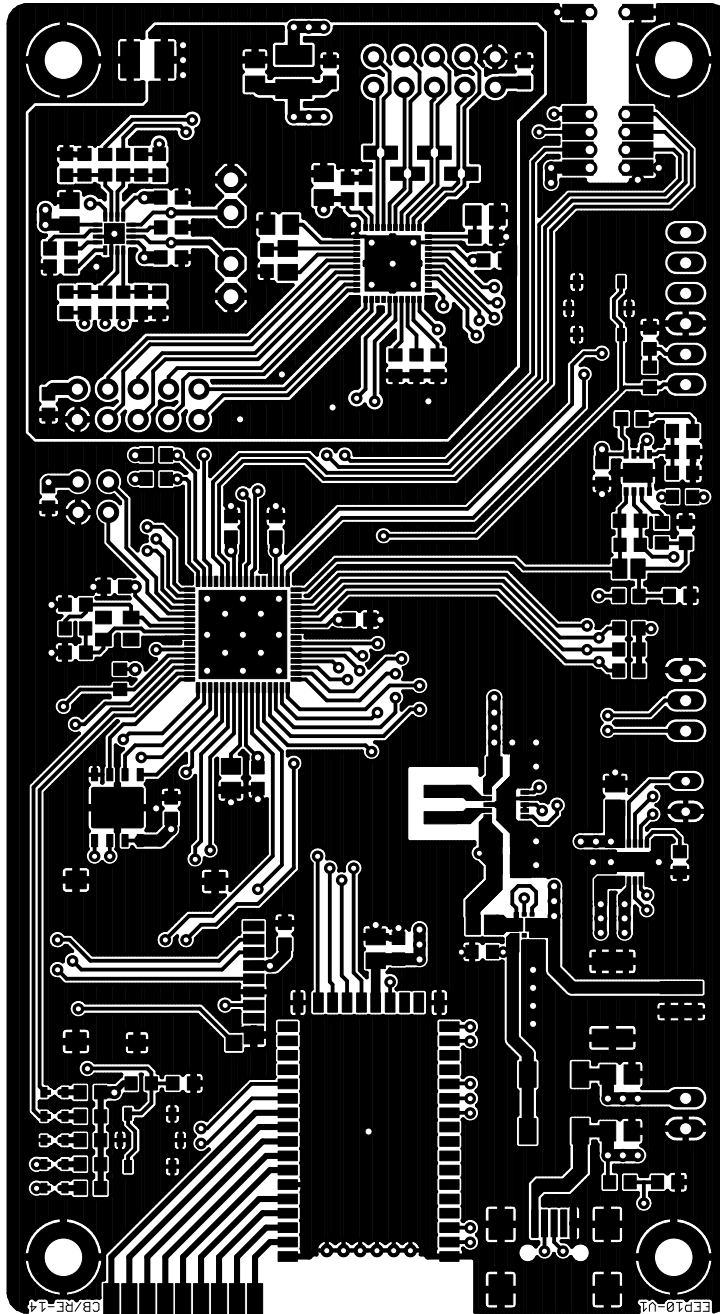
Figure E.2: Main Board top copper layer as seen from top. Image is not to scale.

Main Board Bottom Copper
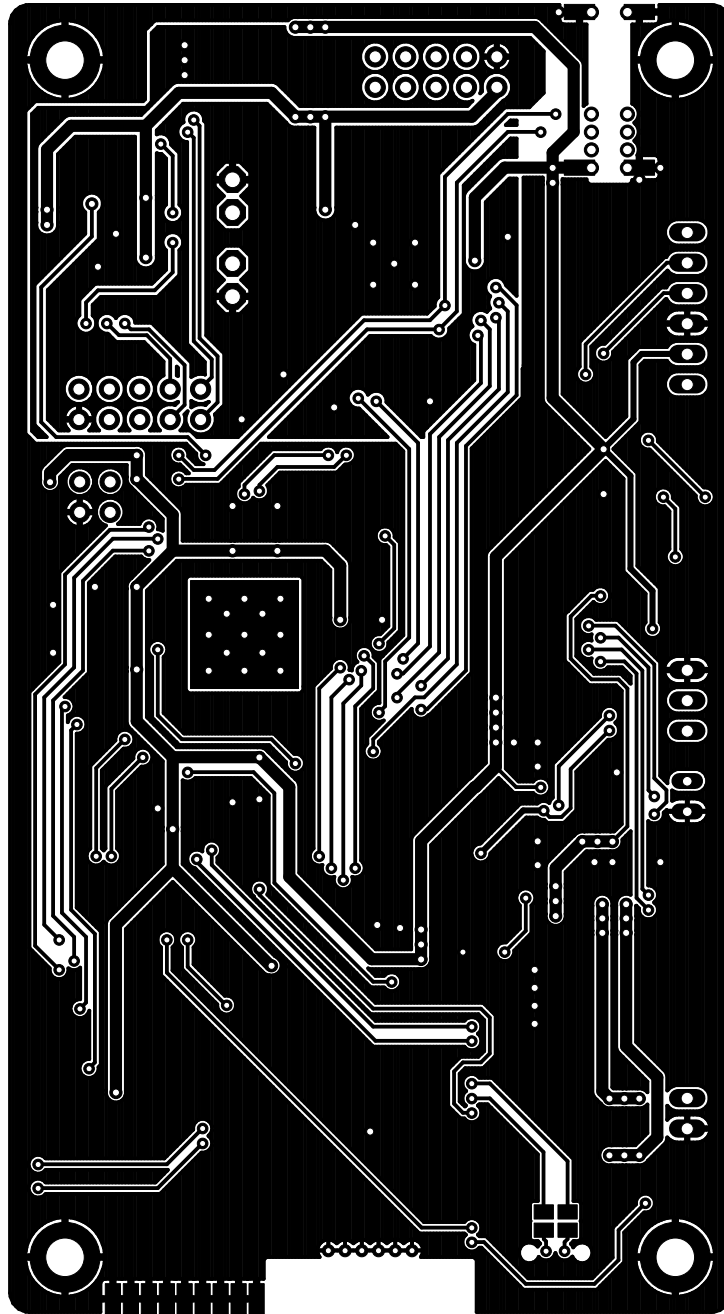
Figure E.3: Main Board bottom copper layer as seen from top. Image is not to scale.

Interface Board Top Copper
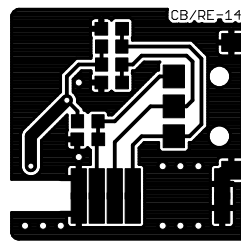
Figure E.4: Interface board top copper layer as seen from top. Image is not to scale.

Interface Board Bottom Copper

Figure E.5: Interface board bottom copper layer as seen from top. Image is not to scale.

Hear Through Top Copper

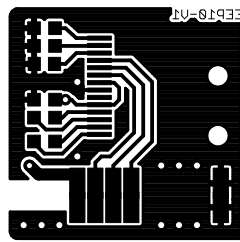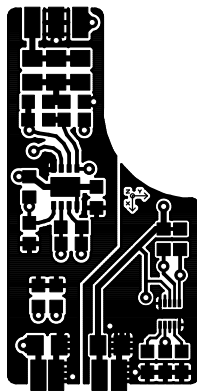**Figure E.6:** Hear through top copper layer as seen from top. Image is not to scale.
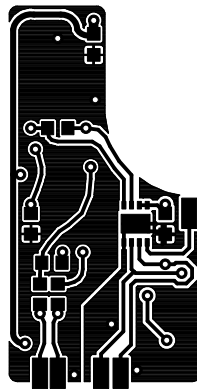
Hear Through Bottom Copper

Figure E.7: Hear through bottom copper layer as seen from top. Image is not to scale.

Pin Mapping Reference

Pin	Type	Name	Periphial	Function
1	O	RP85	DCI	CODEC, TDM DAC data
2	I	/RE6	GPIO	CODEC, Interrupt
3	O	RP87	SPI2	Bluetooth, PCM Frame Sync
4	O	SCK2	SPI2	Bluetooth, PCM Bit Clock
5	I	SDI2	SPI2	Bluetooth, PCM ADC Data
6	O	SDO2	SPI2	Bluetooth, PCM DAC Data
7	I	/MCLR	NA	DSP, Reset
8	NC	-	-	-
9	PWR	VSS	NA	GND
10	PWR	VDD	NA	3.3 V
11	I	RB5	GPIO	Battery Monitor, Status 1
12	I	RB4	GPIO	Battery Monitor, Status 2
13	I	RB3	GPIO	Battery Monitor, Power Good
14	O	RB2	GPIO	Battery Monitor, USB Current
15	NC	-	-	-
16	AIN	AN0	ADC1	Battry Voltage
17	I	PGEC1	NA	Debug Clock
18	I/O	PGED1	NA	Debug Data
19	PWR	VDD	NA	3.3 V
20	PWR	AVSS	NA	GND
21	NC	-	-	-
22	NC	-	-	-
23	O	/RB10	GPIO	Display, Reset
24	I	RB11	GPIO	Switch, Counter Clockwise
25	PWR	VSS	NA	GND
26	PWR	VDD	NA	3.3 V
27	I	RB12	GPIO	Switch, Clockwise
28	I	RB13	GPIO	Switch, Push Button
29	NC	-	-	-
30	O	RB15	GPIO	Headphone Amp. Shutdown
31	OD	SDA2	I2C2	Internal I2C Data
32	O	SCL2	I2C2	Internal I2C Clock

Legend: **O** = *Digital Output*, **I** = *Digital Input*, **I/O** = *Digital Input/Output*, **OD** = *Open Drain output*, **PWR** = *Power Supply Connection*, **NC** = *Not Connected*, **NA** = *Not Applicaple*, **-** = *Unused*, **OSC** = *Crystal Osccilator Connection*

Pin	Type	Name	Periphial	Function
33	O	RP99	SPI3	Micro SD Card, Clock
34	O	RP98	SPI3	Micro SD Card, Slave Select
35	O	RP102	SPI3	Micro SD Card, Serial Data Out
36	OD	SDA1	I2C1	External I2C Data
37	O	SCL1	I2C1	External I2C Clock
38	PWR	VDD	NA	3.3 V
39	OSC	OSC1	NA	System Clock Crystal
40	OSC	OSC2	NA	System Clock Crystal
41	PWR	VSS	NA	GND
42	NC	-	-	-
43	I	RPI73	SPI3	Micro SD Card, Data In
44	I	/RD10	GPIO	Micro SD Card, Card Detect
45	NC	-	-	-
46	O	/RD0	GPIO	System Status LED 1
47	O	/RC13	GPIO	System Status LED 2
48	O	/RE1	GPIO	Flash Memory, Write Protect
49	O	RP65	SPI1	Flash Memory, Serial Data Out
50	I	RP66	SPI1	Flash Memory, Serial Data In
51	O	RP67	SPI1	Flash Memory, Serial Clock
52	O	RP68	SPI1	Flash Memory, Slave Select
53	O	RD5	GPIO	Bluetooth, Power Enable
54	I	RP70	UART1	Bluetooth, UART RX
55	O	RP71	UART1	Bluetooth, UART TX
56	I	VCAP	NA	Internal Logic
57	PWR	VDD	NA	3.3 V
58	I	/RF0	GPIO	Bluetooth, Event
59	O	/RF1	GPIO	Bluetooth, Command
60	O	RP80	DCI	CODEC, TDM Clock
61	I	RPI81	DCI	CODEC, TDM ADC Data
62	O	RP82	DCI	CODEC, TDM Frame Sync
63	O	/RE3	DCI	CODEC, Reset
64	O	RP84	REFCLK	CODEC, Master Clock

Legend: **O** = *Digital Output*, **I** = *Digital Input*, **I/O** = *Digital Input/Output*, **OD** = *Open Drain output*, **PWR** = *Power Supply Connection*, **NC** = *Not Connected*, **NA** = *Not Applicaple*, **-** = *Unused*, **OSC** = *Crystal Osccilator Connection*

Bill Of Materials

Qty	Value	Device	Package	Parts
4		C-USC0603K	C0603K	C58, C59, C60, C61
2	Yellow	LED	LED-TTW	LED1, LED2
1	Red	LED	LED-TTW	LED3
2	Green	LED	LED-TTW	LED4, LED5
1		PINHD-1X6	1X06	JP1
1		PINHD-2X2	2X02	JP7
2		PINHD-2X5	2X05	JP5, JP6
2	8p	C-USC0603K	C0603K	C37, C38
4	2n7	C-USC0603K	C0603K	C43, C44, C45, C46
24	100n	C-USC0603K	C0603K	C1, C8, C9, C10, C11, C12, C14, C15, C17, C19, C22, C24, C25, C26, C27, C30, C31, C32, C33, C48, C49, C52, C62, C63
5	1u	C-USC0603K	C0603K	C2, C23, C53, C54, C56
2	3u3	LQH44PN3R3MP0	1515	L2, L3
12	10u	C-USC0805K	C0805K	C3, C4, C5, C6, C7, C13, C16, C18, C20, C21, C29, C51, C55
5	470	R0603	R0603	R14, R15, R20, R23, R24
1	1k	R0603	R0603	R5
2	2k2	R0603	R0603	R21, R22
17	10k	R0603	R0603	R1, R2, R3, R4, R7, R12, R13, R25, R26, R27, R29, R30, R31, R35, R36, R37, R38
1	14k	R0603	R0603	R40
2	33k2	R0603	R0603	R18, R19
1	47k	R0603	R0603	R39
7	100k	R0603	R0603	R8, R9, R10, R11, R16, R17, R34
1	1M	R0603	R0603	R28

Qty	Value	Device	Package	Parts
1	22.5792 MHz	CX3225GB	CX3225GB	Y1
1	CS4244	CS4244	40QFN	U4
1		DSPIC33EP512GP806	64QFN	U3
2	EVQ-PLHA15	Button	PWB	B1, B2
1	2.2uH	LQH3NPN	1212	L1
1	MAX97220A	16QFN	Line Driver	U12
1	MCP73837	10DFN	Battery manager	U2
1	MICROSD	MICROSD		X3
1	NTC640	P640	NTC	R6
2	PMEG3010EP	SOD128	Schottky Diode	D1, D4
1	PMFPB8032XP	DFN2020-6	Mosfet	U8
1	RN52	RN52	Bluetooth module	U11
1	S2B-PH-SM4-TB	SM4	Battery connector	X2
1	SST25VF032B	8WSON	Serial Flash	U6
1	TPS63001	10DFN	Switcher	U5
1	TS972	8DFN	TS972, op-amp	U9
1	USB-MINI-B	MUSB		X1